University of Alberta

Characterization of Mature Fine Tailings in the Context of its Response to Chemical Treatment

by

Mohammadreza Salehi

A thesis submitted to the Faculty of Graduate Studies and Research

in partial fulfillment of the requirements for the degree of

Master of Science

in

Chemical Engineering

Chemical &Materials Engineering

Fall 2010

Edmonton, Alberta

Examining Committee

Dr. Zhenghe Xu, Chemical and Materials Engineering

Dr. Jacob Masliyah, Chemical and Materials Engineering

Dr. Jozef Szymanski, Civil and Environmental Engineering

To my dear family:

Zafireh, Bahram and Alireza

Abstract

Continuous accumulation of Mature Fine Tailings (MFT) is a major challenge to oil sands industry. To reduce the inventory of MFT through development of novel tailings treatment technologies, it is essential to understand the stabilization mechanism of fine solids in MFT. This project aims at characterizing fine solids of MFT. A novel method is developed in this study to understand characteristics of fine solids in MFT by studying their response to the changes in water chemistry and chemical treatment. Settling and rheological response of MFT to chemical additives is determined. Combined with solids characterization of the different layers of settled MFT, an enhanced understanding of stabilization of fine solids in MFT is gained. The knowledge generated through this study will provide a scientific basis for technology development of MFT treatment.

Table of contents

List of tables

List of figures

1 Introduction

There are two processes for bitumen production: open pit mining and in_situ production. Open pit mining method is implemented for the oil sands deposit shallower than 75 meters and in_situ extraction is used for deeper deposits. A schematic view of the bitumen extraction for open pit mining operation is shown in Figure 1-1.

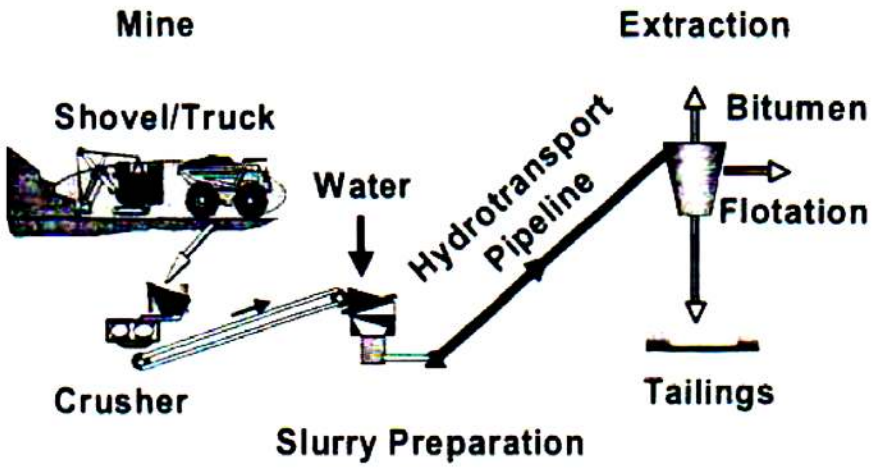

Figure 1-1 Schematic of bitumen production in open pit mining operation [1]

In open pit mining operations, oil sands ore is mined by shovels and crushed, then mixed with water and additives in slurry preparation equipment. The bitumen is liberated under mechanical shear in hydrotransport pipeline. Gravity separation vessels and flotation cells are then used to recover aerated bitumen as bitumen froth. The waste from the extraction process, which mainly consists of water and solids leftovers, is sent to the tailing ponds for dewatering treatments. Two tonnes of oil sands are normally required to produce one barrel of synthetic crude oil thereby much waste is produced for each barrel of synthetic crude oil.

Increasing demand for oil has resulted in an increase in bitumen production from the oil sands. That in turn has created significant challenges and issues to be overcome and addressed. Figure 1-2 illustrates some of the parameters which affect oil sands development.

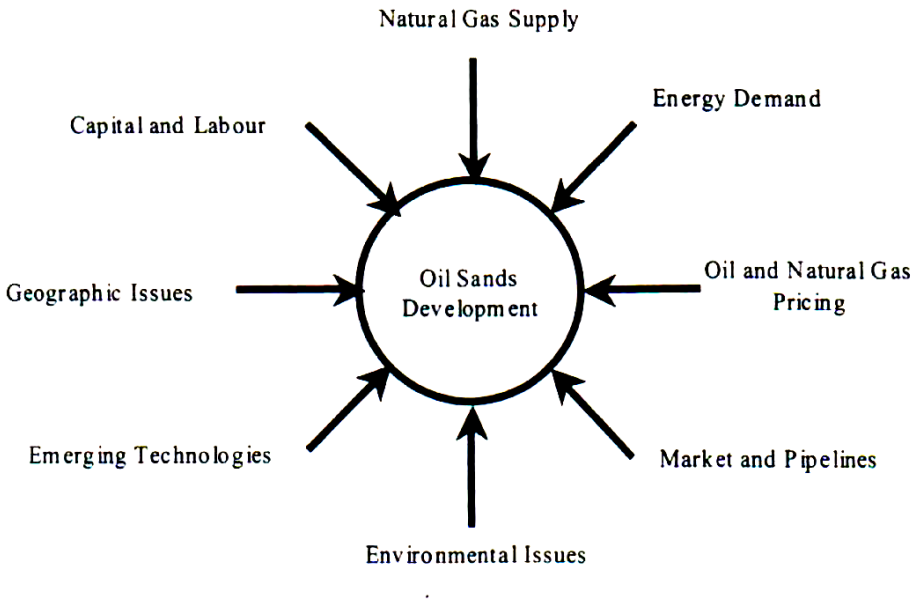

Figure 1-2 Driving forces in oil sands development [1]

A major challenge in environmental issues of oil sands is the water consumption and tailing ponds. The demand for raw water in bitumen production is increasing due to increasing production of existing oil sands operations and the development of new open pit mining plants in Fort McMurray area in Alberta, Canada. This increase in water consumption may limit the production capacity in near future. Another problematic aspect of this subject is the no discharge policy in bitumen production which results in the formation of tailing ponds as the containers of accumulated tailing slurries. In 2007, a total of 16.5 barrels of water were required for production of one barrel of Syncrude Sweet Blend. In general 15% of the needed water in oil sands industry is withdrawn from the raw water sources and

the remaining is from the ponds' recycled water. Figure 1-3 shows the historical water utilization for Syncrude between years 2000 to 2008 [1].

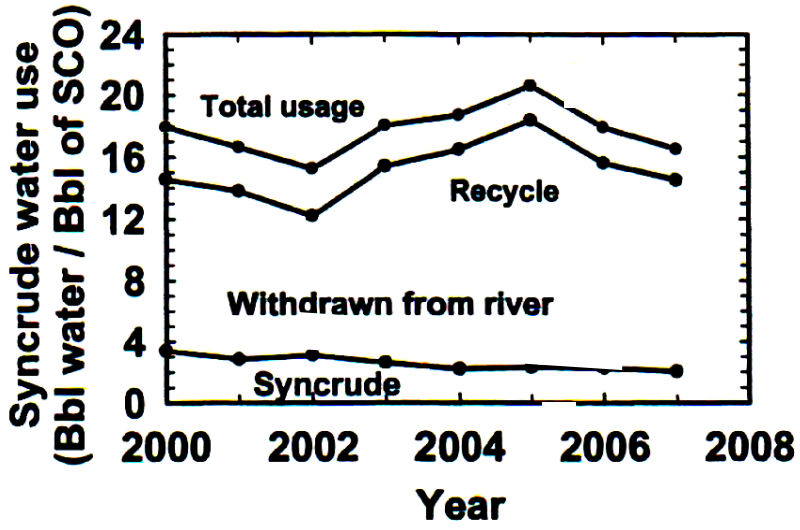

Figure 1-3 Historical water usage at Syncrude [1]

2 Literature review

2.1 Tailing ponds

Tailing ponds have caused much environmental concerns. The rate of increase in tailing ponds' volume is about 0.1 m^3 per tonne of processed oil sand and the growth of mature fine tailings' volume is about 0.06 m^3 per tonne of processed oil sand [2]. With the limitations in the amount of water withdrawal from the river, there is a tremendous pressure to find novel ways of managing the tailing ponds and recycling the water back to the extraction process. Currently 0.75-1 m^3 of recycle water is used for bitumen extraction per tonne of oil sand and about 0.25-0.3 m^3 recycle water is needed for upgrading and utility process plants for same amount of oil sand [3, 4].

Continuous recycling of the process water increases the concentration of salts in tailings water, which could theoretically eventually reach the concentration of salt in the connate water. The effect of these changes is discussed in the section on water chemistry later in this Chapter.

2.1.1 Tailing ponds' containment

Combined streams from the separation vessel, floatation cells and froth treatment are discharged into the tailing ponds. The coarse fraction which segregates rapidly is used to build dykes. The less coarse fraction then settles on the beach as it flows into the tailing ponds. Fine particles settle slowly to form the fine tailing zone and after two to three years of settling the mature fine tailings are formed, which settle very slowly, if they settle at all, due to the presence of ultra fine solids (<0.5 μm) which cause gelation in the slurry. The natural sedimentation of solids will form a solid concentration gradient along the depth of the ponds. The amount of hydrocarbon bounded to the solid particles, on the other hand has a parabolic distribution along the depth, like the one shown in Figure 2-1 .

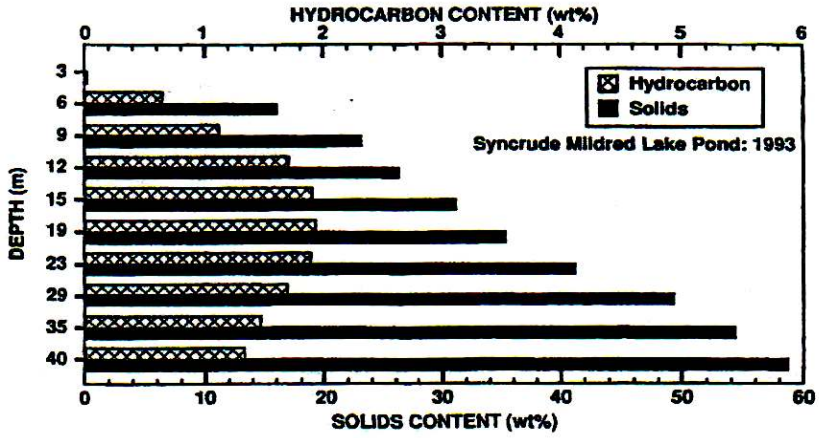

Figure 2-1 Solids and hydrocarbon concentration in different depth of Syncrude tailings pond [5]

The size of the particles changes along the depth of the pond. The particles at a depth of 6 m or less from the surface are finer than 5 µm. While particles at a depth of 40 m or more are larger than 150 µm [5].

Management of the tailing ponds would be easier in the early stage of the operations. After the introduction of new technologies such as composite tailings (CT) and paste technology along with continuous accumulation of tailings several new tailings ponds for CT deposits have to be constructed. Managing this vast amount of slurry seems to be much more complex nowadays. Figure 2-2 shows a schematic comparison between the layouts of the Syncrude tailings ponds during the time interval of 1978-1988 and the period after the year 2000 [5].

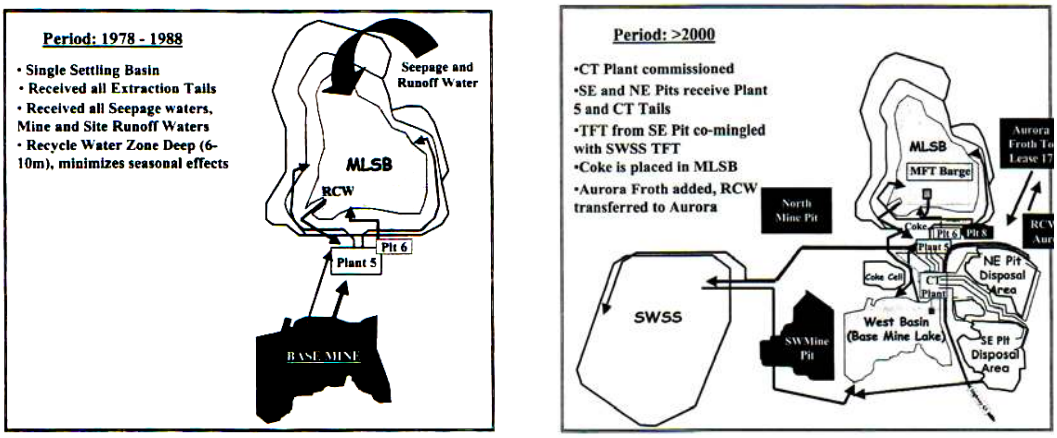

Figure 2-2 Syncrude tailings ponds layout between years 1978-1988 (left) and after 2000 (right) [5]

2.2 MFT formers

Mature fine tailings are formed after two to three years due to the slow sedimentation of fine solids in fine tailing zone. After reaching certain solid concentration MFT slurry becomes stable and forms a gel which entraps both coarse and fine solids in a network, thus no further consolidation would occur. One should seek the reason for such behaviour by analyzing both the liquid and solid phases. The solids characterization and analyses are described below.

One of the most important and problematic properties of MFT is its water holding capacity. About 60-70 wt% of the MFT consists of water which is trapped in the network of fine particles. Yong and Sethi [6] suggested that the specific volume of fine tailings is the weighted sum of the specific volume of its constituents. Among these compounds "Iron-Organic complex" was known to be responsible for water holding capacity of MFT [7, 8]. Allan and Sanford [9] also suggested that ferric ions cause the binding of organic matter to the clays thus affecting their surface properties.

However, subsequent studies illustrated that specific compounds such as iron complexes are not responsible for high water holding capacity in MFT. Numerous researchers have emphasized the importance of the ultra fine clays in MFT

gelation and its high water holding capacity [10, 11]. More detailed discussion in such a shift in theory will be presented later in this section. In order to improve the understanding about the MFT settling behaviour, one should analyze different fractions of solids. For this purpose MFT should be fractionated to different solid fractions (layers) according to the size and settling rate of particles. An example of such a fine tailings fractionation process is illustrated in Figure 2-3 [8]. In this separation method MFT is agitated and centrifuged in different steps. Agitation breaks the gel-like structure of MFT which has thixotropic properties i.e. it is a shear thinning slurry which loses its strength as it is under shear mixing and restructures when the shear is stopped [12]. The gel-like network of the particles, which entraps both fine and coarse solids breaks down upon mixing but restructures fairly fast that the coarser particles do not segregate from the slurry. As a result, the MFT becomes unchanged cession of mixing. Centrifuging the sample after mixing helps the segregation of particles. In this case, sedimentation rate of particles gets faster thus they can escape being trapped in the network and settle.

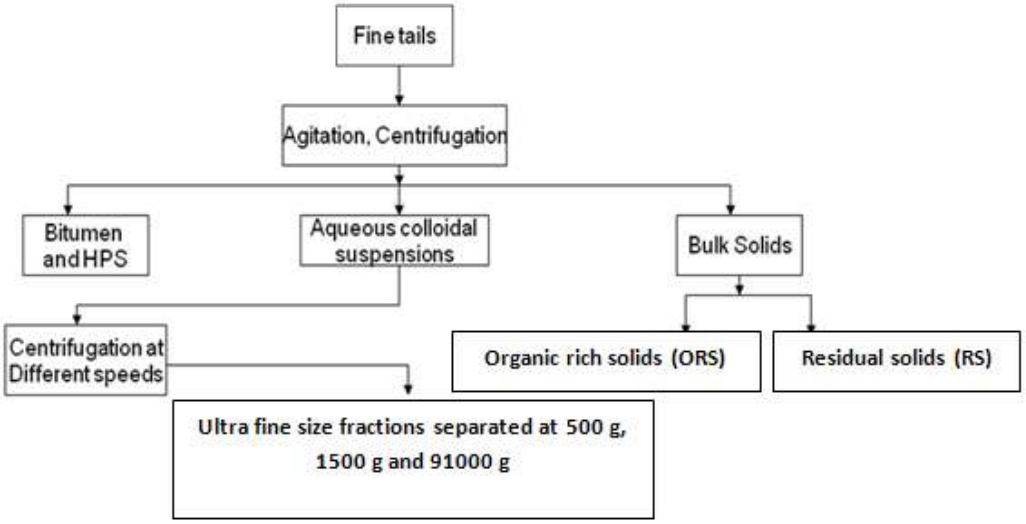

Figure 2-3 Schematic diagram of an example MFT fractionation [8]

In this type of fractionation four distinct layers are observable as depicted in Figure 2-4:

(a) a bitumen layer containing hydrophobic solids (HPS) on the top;

(b) an aqueous colloidal suspension which contains hydrophilic ultra fine solids (HUS) and bi-wetted ultra fine solids (BUS);

(c) a dark color layer in the sediment known as organic rich solids (ORS);

(d) a light color sediment of coarser solids known as residual solids (RS).

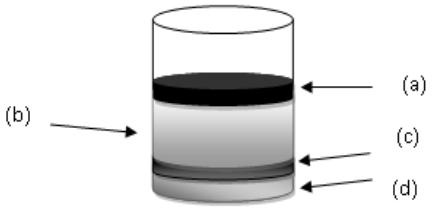

Figure 2-4 Four layers formed by fractionation of bulk fine tailings by agitation and centrifugation [8]

A typical distribution of various fractions from Syncrude and Suncor fine tailings is shown in Figure 2-5.

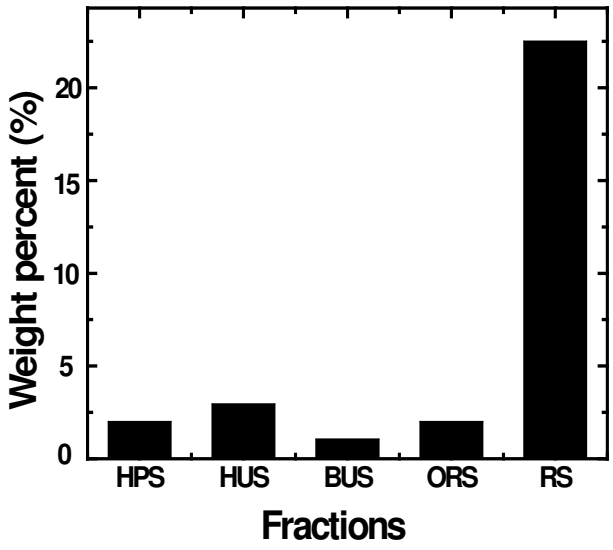

Figure 2-5 Typical composition of solids in whole MFT from Syncrude and Suncor [8]

2.2.1 Hydrophobic solids (HPS)

HPS exist in bitumen layer. About 20-50 wt% of these solids contains organic carbon. Up to 14 wt% of HPS solids contains titanium [13]. In high concentration the solids containing titanium reduce the bitumen recovery in extraction process, but they do not play a major role in water holding capacity of MFT.

2.2.2 Hydrophilic ultra fine solids (HUS) and bi-wetted ultra fine solids (BUS)

Colloidal suspension contains two types of ultrafine solids: hydrophilic ultra fine solids (HUS) and biwetted ultra fine solids (BUS). These types of solids are known to be responsible for gel formation in MFT. The particles in this fraction are of sizes between 0.02 to 0.3 μm. The BUS particles contain strongly bounded organic material (SOM). When they are introduced into a two phase liquid system of water and toluene, they form a layer between the two immiscible phases and thus are known as bi-wetted solids [14]. The HUS on the other hand are hydrophilic, and reside in water.

As mentioned earlier the amount of ultra fine particles is an important factor in water holding capacity of MFT. These ultra fine nano-particles have been characterized by a few researchers. Majid et al. [15] suggested that the amorphous material in the fine particles contains allophones, halloysite, ferrihydrite and amorphous silica. They also reported that the crystalline fraction of these fine particles consists of muscovite and trace of quartz. The fractions of amorphous solids (ASs) were separated by selective dissolution methods. These methods depend on high surface area and low thermodynamic stability of poorly ordered materials which lead to higher dissolution rate than that of crystalline materials. Tiron or NaOH might be used to dissolve the minerals. All ASs feature a high organic matter content, which shows the interaction between the organic matters and inorganic minerals in these solids. Cation exchange capacity (CEC) values for these types of solids are between 14 to 37 cmol kg^{-1} (centimoles of charge per

kilogram) which is in the range for allophones and halloysites. Another property of these solids is the increases in their iron content with decreasing the specific surface area of the particles, which implies an important role of iron compounds in agglomeration of solid particles. Figure 2-6 shows typical XRD patterns of fine and coarse particles. The broader peaks of noise background in the case of fine solids indicate the amorphous nature of them. Dominant minerals in fine particle fraction appear to be muscovite and halloysite. This type of XRD pattern also suggests the presence of allophone type material which could be a reason for the existence of considerable amounts of humic matter, as allophones are strong adsorbents of humified materials. The high level of organic matter is common in soil of high allophone content [16]. The XRD pattern of coarse solids suggests quartz and kaolinite as main solid phases.

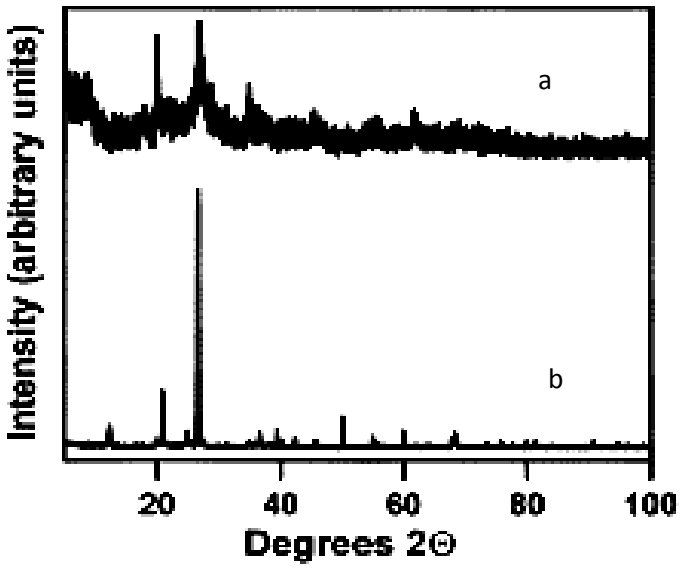

Figure 2-6 XRD patterns for (a) fine and (b) coarse particles [15]

A typical fourier transform infrared spectrometer (FTIR) spectrum of fine and coarse solids is shown in Figure 2-7. In the FTIR spectrum of fine particles the broad absorption around the wavenumber of 3300 cm^{-1} is related to the OH bonds and indicates the presence of amorphous aluminosilicates such as allophones. The strong absorption in the range of 900-1000 cm^{-1}, which is related to Si-O bonds

confirms the presence of such compounds. Absorption in the range of 3600-3700 cm^{-1} is mostly related to halloysite.

The FTIR spectrum of coarse particles on the other hand shows sharper peaks around 3700 to 3600 cm^{-1} which indicates the presence of crystalline minerals. This pattern suggests the presence of kaolinite in coarse particle fraction. The peaks in the range of 780-800 cm^{-1} arise from quartz.

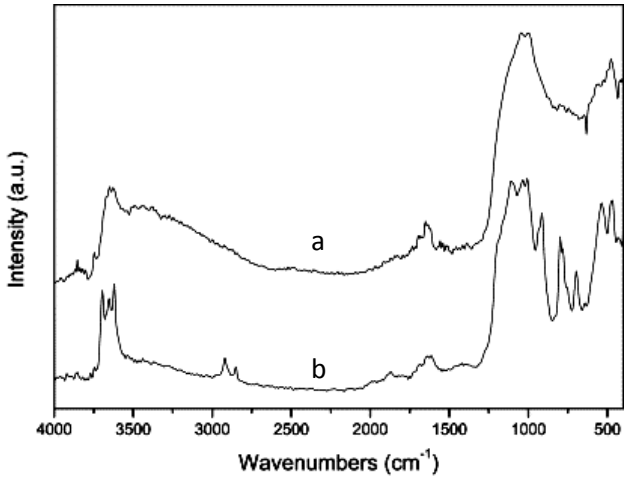

Figure 2-7 FTIR spectrum of (a) fine and (b) coarse particles [15]

2.2.3 Organic rich solids (ORS)

ORS are particles with a size range of 0.5 to 45 μm. These dark colored solids are found between the residual solids (RS) and suspended ultra fine solids (HUS and BUS). Removal of organic matters by means of low temperature plasma oxidation causes disintegration of particle aggregates formed by this type of solids [17]. Though organic rich solids (ORS) are less than 2 wt% of the total solids in the tailings they contain about 30-65 wt% of the total iron content. This finding shows that "iron-organic complexes" are not responsible for water holding capacity of MFT as they settle down (layer (c) in Figure 2-4) and are not present in the aqueous colloidal suspension in layer (b).

2.2.4 Residual solids (RS)

RS account for about 90 wt% of solids in MFT with particles distributed between 0.3 to 45 µm. These solids are not an important factor in gel formation of MFT but they occupy considerable space within the gel network.

2.3 Conventional treatments of MFT

2.3.1 Composite tailings, CT

Composite tailings (CT) process was developed to treat MFT and is commercially used. In a CT process coagulants such as gypsum are added to the slurry of a specific solid to fine ratio. MFT slurries have their characteristic boundaries known as segregation boundary. The solid line in Figure 2-8 shows the percentage of solids as a function of their fines content above which the slurry becomes non-segregating. In other words, all points with solid to fines ratio located above this line will form non-segregating tailings. The term of non-segregated tailings refers to the settling of coarse and fine solids as one unit, in contrast to segregating tailings in which coarse solids settle to the bottom of sedimentation basin and become separated from fines which remains suspended in the water.

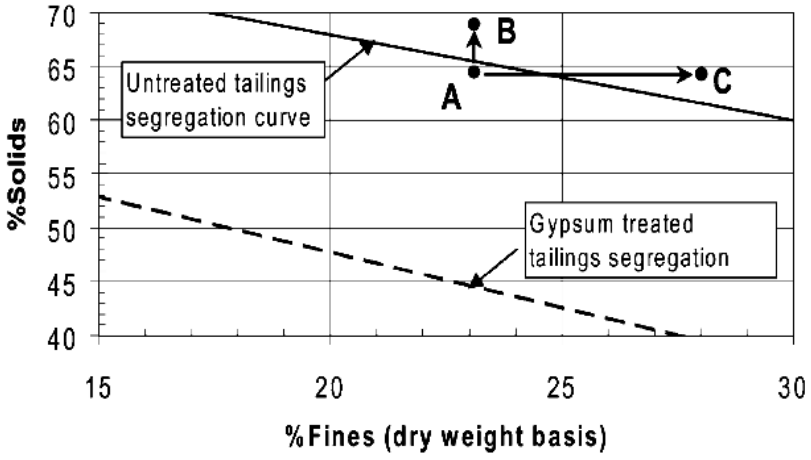

Figure 2-8 Segregation curves for raw and gypsum treated CT slurry [18]

The three basic ways to treat the slurry via composite tailings as shown in Figure 2-8 are:

(a) Increasing solid content from its original amount (point A) to a higher value (point B) by hydrocyclone densification.

(b) Enriching the fine content by mixing the slurry with settled fine tailings to shift the slurry to point C.

(c) Chemical addition of coagulants. In this case, the segregation boundary shifts to lower values of solid content as shown by the dotted line in Figure 2-8, which is the basis of non-segregated CT process [18].

2.3.2 Paste technology

Paste technology has been investigated as a treatment method mainly for fresh tailings i.e. recently discharged tailings which are non-aged or diluted mature fine tailings. In this method, high molecular weight, medium charge anionic polymers, such as partially hydrolyzed polyacrylamide (Percol) have been used for flocculation of fine particles. A detailed discussion on the flocculation mechanism using polymers will be presented in the next section. Studies conducted by Cymerman et al. [19], showed a successful dewatering of MFT by a continuous thickener. Based on results from earlier studies, paste technology was developed as depicted in Figure 2-9, where beach run-off water and fine tailings are combined and introduced into a thickener in which a proper dosage of anionic polymer is added. The overflow water from the thickener is then recycled back to the extraction plant and the underflow in the form of paste is pumped to the sand beach.

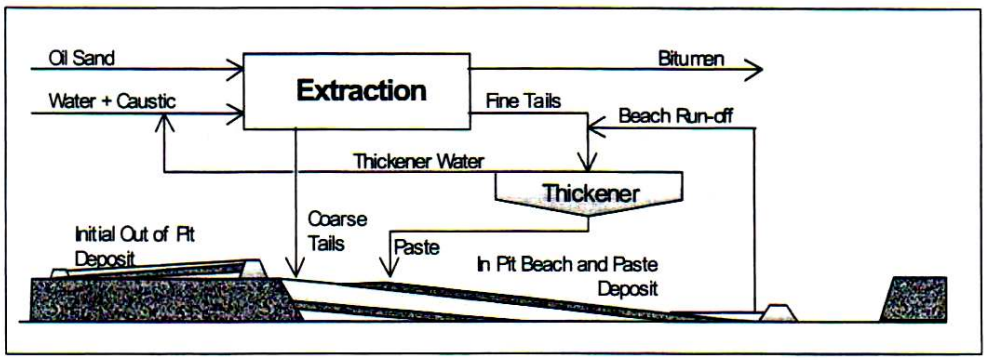

Figure 2-9 Schematic diagram of paste technology [20]

2.4 Flocculation mechanisms

In solid-liquid separation, flocculation of solid particles is one of the most common techniques used in a wide range of industries such as minerals processing, paper manufacturing, water and waste water treatment and tailings dewatering. Inorganic materials as well as cationic, anionic and non-ionic polymer macromolecules have been used as the flocculants [21]. Flocculation of particles occurs via three major mechanisms: bridging, charge neutralization and electrostatic attraction of patch models. It is important to note difference between flocculation by polymer bridging and coagulation by charge neutralization. In birding mechanism, loops and tails of a polymer macro molecule attach to two or more particles and bring them together. Charge neutralization mechanism acts on particles by compressing their electric double layer and thus reducing the repulsion between the particles which eases their flocculation. Inorganic coagulants also work with same mechanism. Electrostatic patch models occur when particles have low charge density and polymer macromolecules have the opposite charge with high charge density. In this case, the net charge of the polymer patch on the surface of one particle causes the particle to attach to the bare part of an oppositely charged particle [22].

2.4.1 Flocculation stages

Flocculation is a complex system involving a number of stages [23]:

(a) Particle-polymer mixing

(b) Attachment of polymer molecules onto particle surfaces

(c) arrangement of the polymer molecules on the particle surfaces

(d) Particle flocculation

(e) Floc breakup due to shear mixing

The aforementioned stages occur simultaneously, and often compete against each other. One of the most important parameters affecting the flocculation is the time scale of each of these stages. Other parameters such as mixing, polymer molecular weight, charge density and dosage of polymers, background electrolyte as well as particle concentration and size are also important in the flocculation of the solid particles. These effects will be discussed in detail in this section.

Understanding the properties of the flocs is crucial in solid-liquid separation processes as different types of flocs are suitable for different separation processes. For example in filtration strong and porous flocs are preferred. The degree of the strength and compactness of a floc can be measured by a parameter known as mass fractal dimension. It is known that particles which form aggregates in a dilute suspension have specific mass fractal characteristics known as mass fractal dimension, D_f [24, 25]. Equations 2.1 and 2.2 show the dependence of the floc mass and density on the mass fractal dimension.

$$M(R) \propto R^{D_f} \qquad \text{Eq 2.1}$$

$$\rho(R) \propto R^{D_f - 3} \qquad \text{Eq 2.2}$$

in which M is the mass, ρ is the density, and R is the radius of the floc. D_f, the mass fractal dimension, has a non integer value between 1 to 3. A solid sphere has a D_f of 3. In any case of porous aggregates D_f is smaller than 3.

To measure the mass fractal dimension, D_f, the static light scattering experiment is conducted. A beam of light is directed on the sample and the intensity of the scattered light (I) is measured as the function of the magnitude of the scattered vector (Q). The following relation exists between these two parameters [26].

$$I(Q) \propto Q^{-D_f} \qquad \text{Eq 2.3}$$

Where $I(Q)$ is the scattered intensity from the aggregate and Q is the wave vector defined as

$$Q = \frac{4\pi n \sin(\theta/2)}{\lambda} \qquad \text{Eq 2.4}$$

in which n is the refractive index of the fluid, λ is the wavelength in vacuum of the laser light used, and θ is the scattering angle.

2.4.2 Effect of polymer dosage and charge density on flocculation

Varying the dosage of the polymer has direct effect on aggregate size and structure, and hence initial settling rate. The adsorption of the polymer on the surface of the clay occurs via stages outlined below:

(a) Removal of some solvent from solvated polymer, which requires energy as the polymer is initially soluble.

(b) Some bare space on the surface of the particles must be provided. This process needs energy because this is a dewetting process.

(c) The polymer then gets adsorbed on the particles and loses its freedom of motion.

(d) Releasing surface energy as the adsorption process is spontaneous.

For a given solid suspension, the rate of polymer adsorption depends on polymer molecular weight and concentration, type of solvent and temperature [5].

Figure 2-10 shows the initial settling rate of MFT slurry as a function of polymer dosage. Among the four medium charge density, anionic copolymers of polyacrylamide and acrylates with different molecular weights, known as Percol, Percol 727 of the highest molecular weight and medium charge density leads to the highest initial settling rate [19].

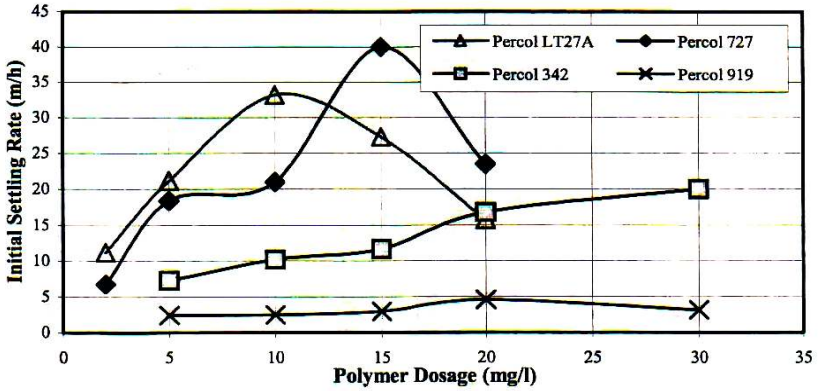

Figure 2-10 Initial settling rate for four types of flocculant [19]

This figure shows that for Percol 727 and Percol LT27A, there is an optimum polymer dosage where the initial settling rate is highest. The reason for the hindrance of the settling after the optimum dosage is the steric stabilization of the slurry [5].

Polymer dosage and charge density have an important effect on the floc structure. The determining parameter in the size and degree of the compactness of a floc is the polymer conformation on the surface of the particle. Polymer can be adsorbed on particle surfaces either in the extended loops and tails or flat polymer patch conformation. In the first case, branches of the polymer protrude from the surface while in the second case, most of the polymer branches are attached to the surface and only a limited number of polymer branches are extended out of the particle

surface. Polymer dosage has a profound effect on this conformation. To further investigate this effect, a case study is presented here. Two cationic polymers with charge densities of 10% and 100% and molecular weights of $3\times10^5$and 1.2×10^5 were used to flocculate 90 nm silica particles. Figure 2-11 shows the flocs size and D_f of flocs formed at different polymer dosages for these two types of polymers.

At any specific dosage of the polymer it is possible to calculate the number of polymer molecules per particle. Knowing the hydrodynamic diameter of the polymer molecule one can calculate the maximum number of polymer molecules adsorbed on a surface of 90 nm silica spheres. This number for the aforementioned polymers with charge densities of 10% and 100% is 8 and 7, respectively. Thus, if the number of polymer molecules per particle in the suspension is higher than this maximum number, polymer molecules will have tail and loop conformation, whereas if the number of polymer molecules per particles is lower than this maximum number, the conformation will be flat polymer patches.

The other important parameter determining the degree of the compactness is the charge density of the polymer, which plays an important role in the electric double layer compression. Figure 2-12 shows the change in zeta potential of silica particles as a function of polymer dosage. As expected, the adsorption of cationic polymer with higher charge density is higher on the negatively charged surface of the silica particles.

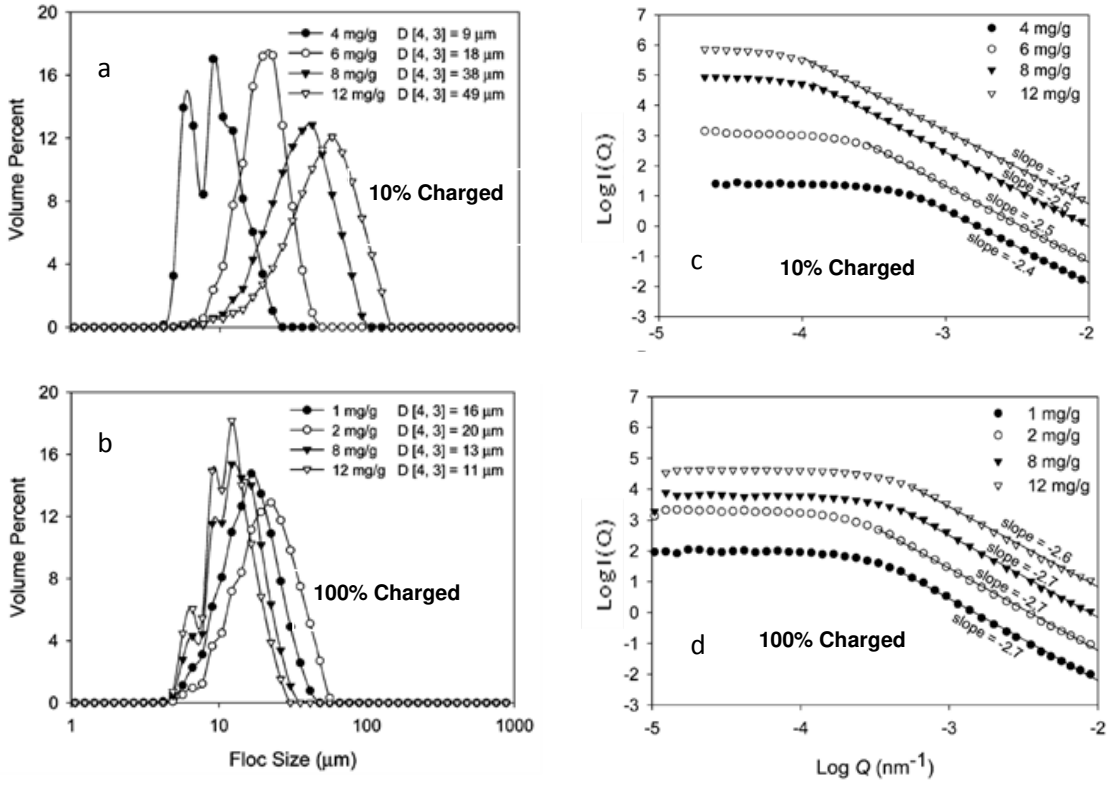

Figure 2-11 **Size distribution (left) and D_f (right) of the flocs formed by addition of two cationic polymers with charge densities of 10%, and 100% to silica particles** [26]

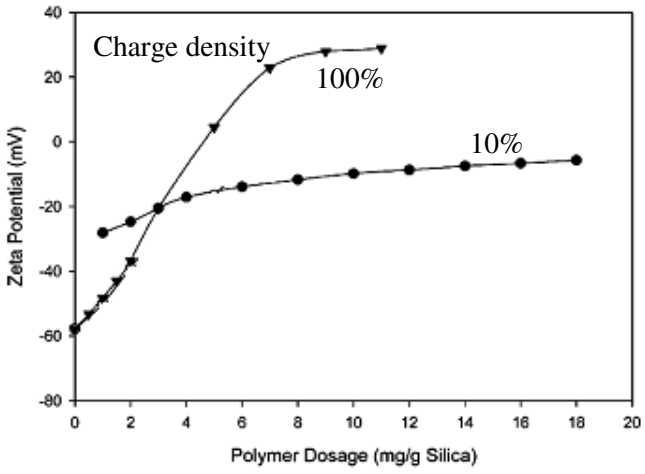

Figure 2-12 **Changes in the zeta potential of silica particles as a function of polymer dosage** [26]

Figure 2-11 (a) shows that for cationic copolymer with charge density of 10% the flocs size increases with increasing the dosage of the polymer from 4 to 12 mg/g. The maximum number of polymer molecules to completely cover the surface in this case is 8, corresponding to a polymer dosage of 6 mg/g. As the polymer dosage increases above this concentration, the flat patch conformation will shift towards the extended tail and loop conformation which leads to an increase in the size of the flocs. Bridging seems to be the dominant mechanism of flocculation in this case. For this polymer, the change in the zeta potential is not significant with increasing polymer dosage as shown in Figure 2-12. Considering relatively low D_f values in Figure 2-11 (c), this finding supports the idea that bridging is the most important mechanism for this system. In the case of cationic polymer with the charge density of 100%, the floc size increases as the polymer dosage increases from 1 to 2 mg/g as shown in Figure 2-11 (b). In this range of polymer dosage, the conformation is flat. The zeta potential in Figure 2-12 does not show significant change in the surface charges of the particles over this low concentration range, indicating that the electrostatic patch mechanism remains to be the only mechanism for the flocculation of the particles. At polymer dosage of 8 and 12 mg/g the extended loop and tail conformation causes the bridging mechanism to be the dominant flocculation mechanism. D_f value is 2.7 for the polymer concentrations of 1 mg/g, 2 mg/g and 8 mg/g. When the concentration of polymer reaches the 12 mg/g D_f value reduces to 2.6 due to presence of tails and loops. The higher D_f values for polymer of 100% cationic charge density (which is about 2.7) in comparison with the polymer of 10% charge density (which is about 2.4) show the formation of stronger flocs in this type of polymer.

2.4.3 Effect of particle concentration on flocculation

Conventional aggregation theory suggests that larger aggregates will form from a slurry of higher solid concentration [27, 28]. Figure 2-13 confirms this theory for

the cationic polymer with 10% charge density, as flocs formed are larger in size from slurries of higher solid concentration.

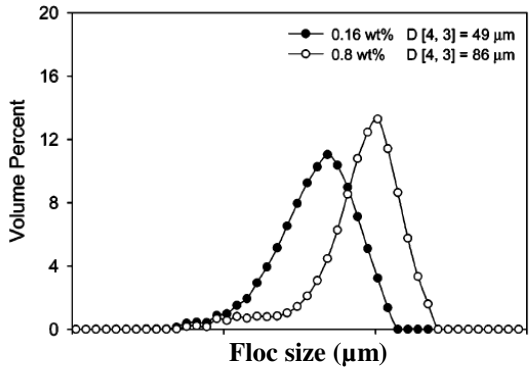

Figure 2-13 Effect of particle concentration on floc size [26]

2.4.4 Effect of particle size on flocculation

Flocculation of ultra-fine particles with different sizes leads to formation of different types of flocs. Kotlyar et al. [11], investigated the formation of the flocs from different sizes of ultra fine particles extracted from MFT slurries using NaCl as the flocculant agent.

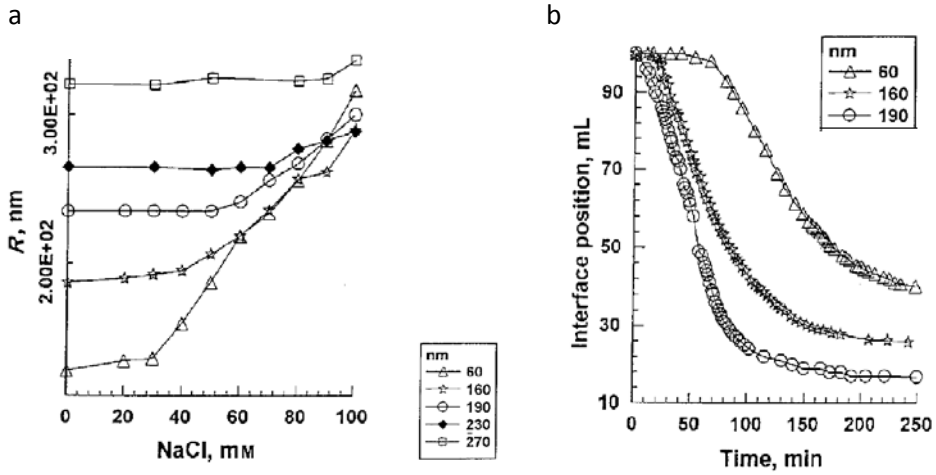

Figure 2-14 (a) mean hydrodynamic radius of flocs and (b) settling of the flocs formed from ultra fine particles with different primary sizes [11]

Figure 2-14 (a) shows the mean hydrodynamic radius of the flocs as a function of NaCl concentration. They suggested that the flocculation value, i.e. the concentration of salt at which a noticeable increase in the mean hydrodynamic radius of floc occurs, increases as the particle size increases. They have also shown that smaller particles form larger flocs with higher water to solid ratios. Figure 2-14 (b) shows that smaller particles settle down slower. Smaller particles seem to have longer induction time i.e. the period before settling gets started [11].

2.4.5 Effect of water chemistry on flocculation

It is well known that the chemistry of water is one of major determining parameters in flocculation of solid particles in MFT. Changes in the pH of the slurry and the concentrations of cations such as magnesium (Mg^{2+}), calcium (Ca^{2+}), manganese (Mn^{2+}), iron (Fe^{+3}) and anions such as chloride (Cl^{-}), hydrogen carbonate (HCO_3^{-}), change the coagulation and flocculation of particles drastically. Sworska et al. [29], concluded that initial settling rate of the particles increases with increasing pH and the supernatant quality would be the best (<0.3 wt%) in acidic pH. Over a low pH range, the optimum initial settling rate and the optimum solid content in supernatant coincide. Hogg [30], also suggested that in alkaline pH flocculation, by addition of polymer results in a bimodal size distribution, consisting of the dispersed fine particles in supernatant and large flocs in the sediment. Hogg has shown that this bimodal size distribution occurs due to the fact that the larger particles receive more polymer per particle than the finer particles [31]. Sworska et al. showed that for a specific initial settling rate, the required dosage of the polymer increases as the pH decreases. They justified their finding by the change in the conformation of the polymer. The carboxylic group of the polymer tend to have a coil structure at low pH, while in high pH they have a more open structure due to the repulsion of negative charges in the carboxylic group. Therefore bridging mechanism is more limited in acidic conditions and higher dosage of polymer is required.

Reduction of pH in MFT treatment does not seem to be the best choice as it is a disadvantage to the extraction process, where the pH of the recycle water should be in the alkaline range. Addition of $Mg^{2+}$and Ca^{2+} to the slurry in alkaline range improves the quality of the supernatant. The optimum dosage and pH for treating the slurry will shift to a lower polymer dosage and higher pH by the addition of cations such as $Mg^{2+}$and Ca^{2+} to the slurry prior to treatment.

Zhou and Franks [26], investigated the effect of background electrolyte on floc formation. They concluded that increasing the salt concentration in the slurry will result in the formation of bigger flocs with lower mass fractal dimension, in cases where flocculation occurs via bridging mechanism i.e. flocculation with polymer of 10% charge density. In contrast in the case of polymer with 100% charge density, the flocculation occurs through flocculation patch model, and increasing the background salt concentration does not have considerable effect on the size and structure of formed flocs.

2.4.6 Effect of mixing on flocculation

Proper mixing is another criterion in successful flocculation. Local over dosing can occur due to poor mixing condition where concentrated flocculant meets the slurry [32].

In sedimentation of MFT slurries, both the initial settling rate and solid content in the sediment are affected by the impeller speed. Figure 2-15 shows this dependency.

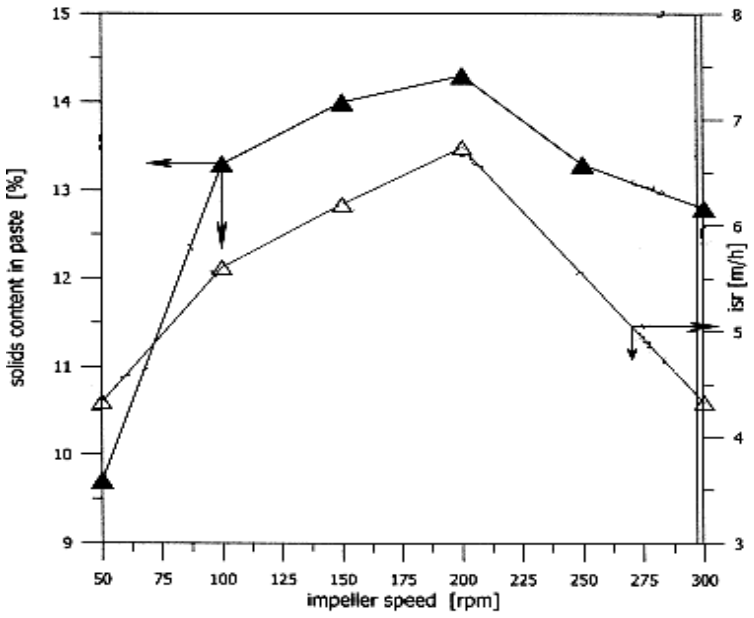

Figure 2-15 Initial settling rate△ and solid content in paste ▲as the function of mixing rate [33]

These results reveal that with increasing the initial settling rate, the solid content at sediment increases accordingly. This figure also indicates the existence of an optimum impeller speed. It was observed that the adequate mixing did not have any effect on the supernatant quality. On the other hand, altering the water chemistry by addition of Mg^{2+} or Ca^{2+} improved the clarity of supernatant but did not have any effect on the initial settling rate and sediment's solid content [29].

An increase in shear rate can increase the aggregation rate as it increases the particle collisions. On the other hand, it increases the breakage of the flocs. It has been observed that the size of flocs flocculated with the two cationic polymers mentioned before, decreases as the shear rate increases. Regarding the structure of the flocs, it has been observed that in the cases where bridging is the dominant mechanism in flocculation, increasing the shear rate increases the D_f , while in the cases where electrostatic patch model is the flocculation mechanism, D_f remains unchanged.

2.4.7 Effect of dilution on flocculation

Dilution results in reduction of solid content. Solid concentration has direct influence on the size of flocs. The solid concentration of the slurry determines the pattern of sedimentation. Solid particles in slurry settle down via three different mechanisms:

(a) Free independent settling of the particles or aggregates which occurs at low solid concentrations. Settling rates are relatively independent of solid concentration in this case and no mud line is visible.

(b) Hindered settling also known as sweep settling where particles and aggregates interfere with the sedimentation of their neighbouring particles and settling rate decreases as solid concentration increases. Large aggregates in this case sweep smaller particles and aggregates to the bottom of sedimentation basin.

(c) Compression, where particles settling rate is restricted by the settled particles below them and dewatering is due to the compaction of the sediment layer.

Banisi and Yahyaei [34], observed the existence of an optimum dilution where the settling rate of the flocculated particles was highest in the samples prepared from the refuse of a coal preparation plant. They also concluded that lower solid concentration results in higher sediment solid concentration. Their results also confirm that higher solid concentration in the original samples causes the formation of larger flocs with a network structure. They claimed that dilution is the key component in successful solid separation in the thickener without which the overflow loses its clarity.

2.5 Novel processes for treatment of fine tailings

So far, none of the treatment methods has been a suitable remedy for MFT challenges. Modification of the conventional recipes such as paste technology

seems to be helpful. Research on other options such as filtration and centrifugation is being conducted. In this section a brief discussion of the aforementioned issues will be presented.

2.5.1 Flocculation modification

It has been observed that conventional single flocculant or single coagulant or a coagulant-flocculant treatment is not effective for slurries of high fines content such as tailings produced by transition ores. Single flocculant treatment for slurries with high content of fine clays will result in solid content of the thickener overflow to be about 1 wt% which will increase to about 5 wt% due to water recirculation [35].

Yuan et al [35], suggested that the sequence of the addition of flocculants and coagulants has a profound effect on dewatering of fresh tailings. They have shown that a coagulation stage followed by a flocculation and again a coagulation stage (CFC) or a flocculation stage followed by a coagulation stage (FC) or (FCF) improved the sedimentation of solid particles drastically and produced a supernatant with a satisfactory clarity i.e. solid content< 0.1wt%. It was also observed that FCF treatment increased the initial settling rate substantially due to the formation of super flocs. They concluded that at least one stage of coagulant addition is needed after flocculation in all aforementioned acceptable processes. The proposed mechanism of the successful FCF method by Yuan et al. is described in Figure 2-16.

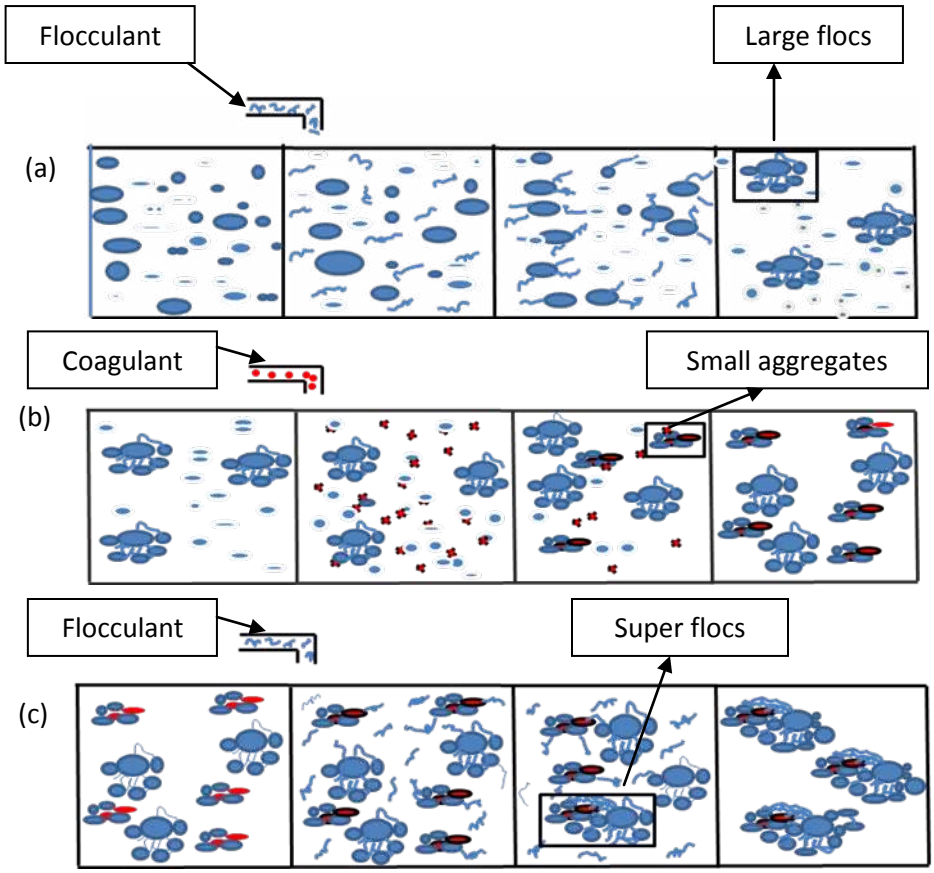

Figure 2-16 Proposed mechanism for the formation of super flocs in FCF method [35]

(a) The flocculant added in the first stage attaches to the larger particles to form large flocs while finer particles remain stable. This results in a bimodal size distribution in the slurry.

(b) The cationic coagulant added binds the fine particles to form small aggregates. This aggregation occurs due to electric double layer compression of negatively charged fine particles. Cationic coagulant can be adsorbed on the surface of small particles due to their low molecular weight, while macromolecule of flocculants can not.

(c) The small amount of flocculant added in third stage binds the small aggregates to large flocs, which results in the formation of super flocs of solid which settle down rapidly.

2.5.2 Centrifugation option

Centrifugation has been successfully used in two pilot plants in Utah tar sands extraction plant. This has led to production of dry stackable tailings, i.e. a mineral stream left from bitumen extraction process which can be stored with no need for containment [36]. The production of dry stackable tailings reduces the water requirement per barrel of extracted bitumen by a factor of two. Mikula et al. [36] suggested that centrifuge would be a proper option for dewatering of Athabasca oil sands fine tailings. They also suggested that a proper dosage of high molecular weight, medium charge density polyacrylamide flocculant should be used as centrifuge aid and significant amount of dilution is needed to efficiently mix the polymer and solid particles.

2.6 Rheological behaviour of MFT

"Rheology" refers to the study of the deformation and flow of the matter. This term was used by Professor Bingham and widely accepted after the formation of American Society of Rheology in 1929 [12]. Rheology covers a wide scope of studies in areas such as biorheology, polymer rheology and suspension rheology. The latter is of particular interest in study of MFT. As mentioned in Section 2.2, MFT shows thixotropic properties. Gelation occurs in MFT under certain conditions which will be discussed later in the present Chapter. Due to gelation the slurry becomes non-segregating and a network is formed between the solid particles which entrap both coarse and fine particles and thus no dewatering will occur. The degree of the gelation can be measured using H NMR method or oscillatory sweep tests which can be conducted by rheometer.

2.6.1 H NMR

When solid particles in the sample are present as a sol i.e. without any structural network among them, the deuterium NMR spectrum gives two distinct peaks with a well defined peak splitting (Δ). As gelation proceeds, peak splitting decreases

until only one peak remains when system is completely gelled. The schematic representation of such a phenomenon is shown in Figure 2-17.

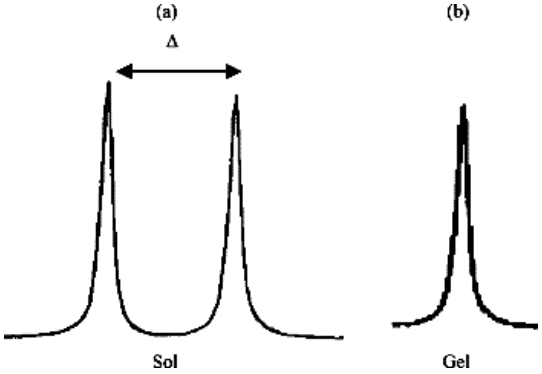

Figure 2-17 H NMR peaks for (a) sol and (b) gel slurries [10]

The rate of gelation can be shown by a parameter known as gelation index I defined by Equation 2.5

$$I = \frac{\Delta_0 - \Delta_t}{\Delta_0} \times 100 \qquad \text{Eq 2.5}$$

in which Δ_0 is the peak splitting at time zero and Δ_t is the peak splitting at time t.

2.6.2 Oscillatory sweep test

2.6.2.1 Linear viscoelasticity

Prior to explanation of oscillatory sweep test a brief introduction to linear viscoelastic properties of materials is crucial. The general differential equation which governs the linear viscoelastic behaviour of materials is

$$(1 + \alpha_1 \frac{\partial}{\partial t} + \alpha_2 \frac{\partial^2}{\partial t^2} + ... + \alpha_n \frac{\partial^n}{\partial t^n})\sigma = (\beta_0 + \beta_1 \frac{\partial}{\partial t} + \beta_2 \frac{\partial^2}{\partial t^2} + ... + \beta_m \frac{\partial^m}{\partial t^m})\gamma \qquad \text{Eq 2.6}$$

where σ is the shear stress and γ is the strain. The coefficients of the time derivatives are constant. Two ideal extremes exist in the deformation of materials. If β_0 is the only non-zero parameter, Equation 2.6 becomes

$$\sigma = \beta_0 \gamma \qquad \text{Eq 2.7}$$

This is the equation of Hookean elasticity, where β_0 is the rigidity modulus. This equation can be modeled with a spring, shown in Figure 2-18 (a). The response in this case is instantaneous i.e. a sudden change in the stress will result in a sudden change in strain. If β_1 is the only non-zero parameter, Equation 2.6 becomes

$$\sigma = \beta_1 \frac{\partial \gamma}{\partial t} \qquad \text{Eq 2.8}$$

This is the equation of Newtonian viscous flow where β_1 is the coefficient of viscosity. This equation can be modeled by a dashpot of Figure 2-18 (b). In fact all materials fall within these two extremes, i.e. they are viscoelastic and in different conditions they can be more liquid like (closer to the Newtonian fluid model) or solid like (closer to the Hookean model). Different models exist to explain viscoelastic behaviour of materials: one of the simplest among them is the Kelvin model. In this case if $\beta_0 (= G)$ and $\beta_1 (= \eta)$ are both non-zero, while all other parameters are zero, Equation 2.6 becomes

$$\sigma = G\gamma + \eta \frac{\partial \gamma}{\partial t} \qquad \text{Eq 2.9}$$

If a stress $\bar{\sigma}$ is suddenly applied at time zero and held constant afterward, one can simply show:

$$\gamma = (\frac{\bar{\sigma}}{G})[1 - \exp(-t / \tau_k)] \qquad \text{Eq 2.10}$$

where τ_k is the ratio η / G and called 'retardation time'. The equilibrium value for γ in this equation will be $\bar{\sigma} / G$, which is the value for the Hookean model. But the response is delayed due to the presence of Newtonian fluid in this case. As the viscosity of the fluid increases this delay time will also increase. These three models are shown in Figure 2-18 [12].

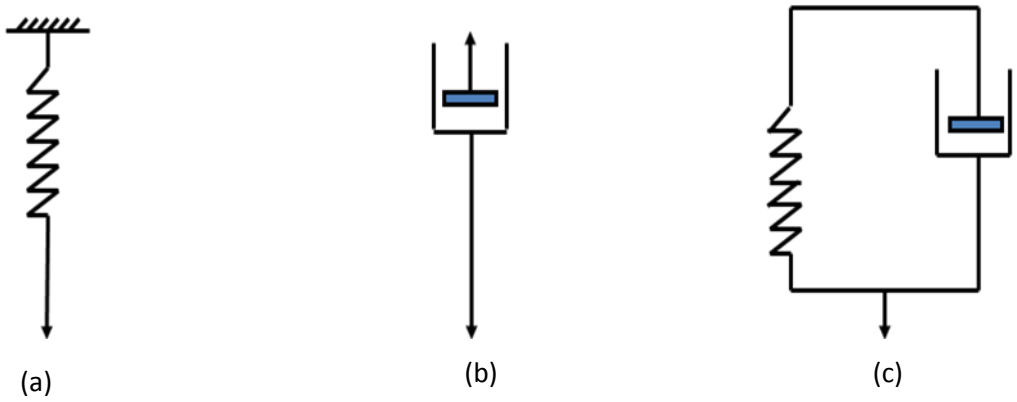

Figure 2-18 Deformation of materials by (a) Hookean model, (b) Newtonian fluid flow model and (c) Kelvin model

2.6.2.2 Oscillatory strain sweep

An important test which is used to understand the degree of gelation of slurries is called strain sweep. In this experiment the sample is deformed sinusoidally with a specific frequency as described by Equation 2.11.

$$\gamma = \gamma_0 \sin \omega t \qquad \text{Eq 2.11}$$

The stress then also oscillates with the same frequency but with a shift by a phase angle δ as described by Equation 2.12.

$$\tau = \tau_0 \sin(\omega t + \delta) \qquad \text{Eq 2.12}$$

The right hand side of Equation 2.12 can be written as:

$$\tau = \tau^{'} + \tau^{''} = \tau_0^{'} \sin \omega t + \tau_0^{''} \cos \omega t \qquad \text{Eq 2.13}$$

Thus the stress wave can be decomposed into two waves of the same frequency, one in phase with the strain ($\sin(\omega t)$) and one 90^o out of phase with the strain ($\cos(\omega t)$).

The phase angle can be calculated from Equation 2.14;

$$\tan\delta = \frac{\tau_0^{''}}{\tau_0^{'}} \qquad \text{Eq 2.14}$$

The decomposition of stress into the aforementioned components in Equation 2.13 suggests the definition of two dynamic moduli;

$$G^{'} = \frac{\tau_0^{'}}{\gamma_0} \quad \text{in phase or elastic modulus} \qquad \text{Eq 2.15}$$

$$G^{''} = \frac{\tau_0^{''}}{\gamma_0} \quad \text{out of phase, viscous or loss modulus} \qquad \text{Eq 2.16}$$

Thus Equation 2.13 can be written as

$$\tau = G^{'}\gamma_0 \sin(\omega t) + G^{''}\gamma_0 \cos(\omega t) \qquad \text{Eq 2.17}$$

And it can be simply understood from the definition of $G^{'}$ and $G^{''}$ that

$$\tan\delta = \frac{G^{''}}{G^{'}} \qquad \text{Eq 2.18}$$

The magnitudes of $G^{'}$ and $G^{''}$ reflect the viscoelastic properties of a solid suspension. Larger $G^{'}$ in comparison with $G^{''}$ indicates more solid like behaviour of the suspension, whereas larger $G^{''}$ in comparison with $G^{'}$ shows the domination of liquid like properties of the suspension. These are important parameters as they show the degree of slurry gelation, which is a crucial parameter in extraction as well as dewatering process [37].

2.6.3 Gelation of ultra fine clays

Ultra fine clay particles (<0.3μm) suspended in the water interact with each other in the presence of cations to produce a sterically stabilized structure. The slurry in this case is Non-Newtonian with thixotropic and shear thinning properties [10].

Kotlyar et al. showed the dependency of the degree and rate of gelation on the size of the fine particles. Figure 2-19 reveals that as the size of particles decreases the degree of gelation (gelation index) increases [11]. It has been claimed that this behaviour is due to the low absolute values of the repulsive potential for small particles [38].

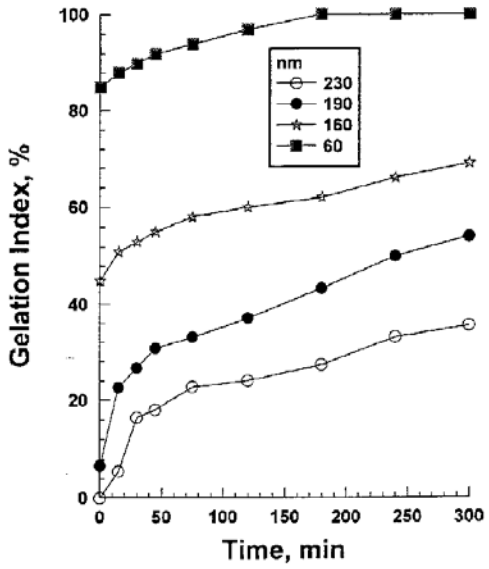

Figure 2-19 Gelation index for particles of different size [11]

Tu et al. [10] showed that the ultra fines and clay contents increase linearly with fines content. They suggested that regardless of the initial ultra fines concentration in the suspension they settle down to a final sediment volume containing 3 wt/vol% ultra fine solid particle. This value is known as the critical gelation concentration (CGC). Thus, if the original concentration of ultra fines is equal or greater than the CGC, gel structure will form and no sedimentation will take place. The rate of gelation is another important parameter both in the primary separation vessel (PSV) and dewatering of MFT. Figure 2-20 shows the rate of change in the gelation index as a function of ultra fines concentration. As expected an increase in the concentration results in increased rate of gelation.

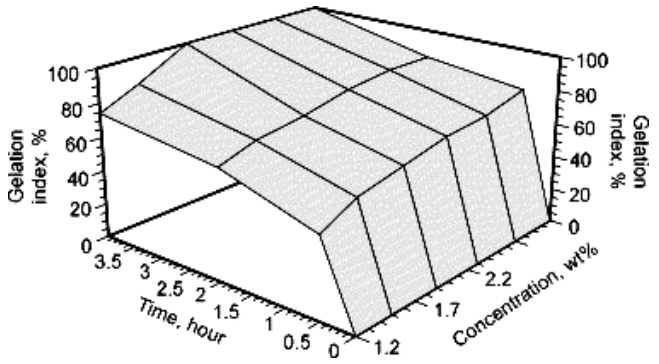

Figure 2-20 Rate of gelation as a function of time and ultra fines concentration [10]

Clay particles (<3µm) also can form gel networks in the suspension but their critical concentration is around 16 wt%, whereas CGC for ultra fines is about 1.5 wt%.

2.6.4 Elasticity of different layers of clays

Angle et al. [39], showed that after ultracentrifugation of MFT different layers of solids are observed in the centrifugation tube and these layers exhibit different elasticity. They separated a whole MFT sludge into three layers of solids by ultracentrifugation as depicted in Figure 2-21. The top layer was the bitumen rich layer. The point of focus in their work was the middle and bottom layers with median size of 19.6 µm and 13.2 µm, respectively.

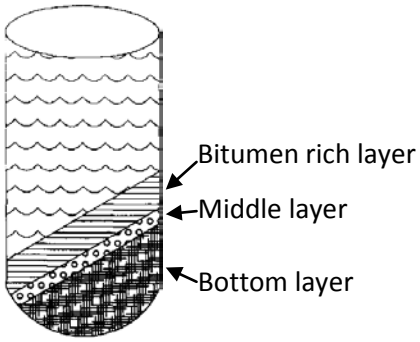

Figure 2-21 Three layers of solids separated by ultra centrifugation [39]

The FTIR analysis showed the presence of a higher amount of organic material and lower amount of minerals in the middle layer than in the bottom layer. The

oscillatory sweep tests for middle and bottom layers as well as reconstituted middle plus bottom layer revealed the elastic properties of these two distinct layers. Figure 2-22 shows the elastic modulus of sludges before shearing (original), after flocculation due to mixing and after deflocculation due to excessive mixing. All samples had the same solid concentration of 10.42 vol/vol%.

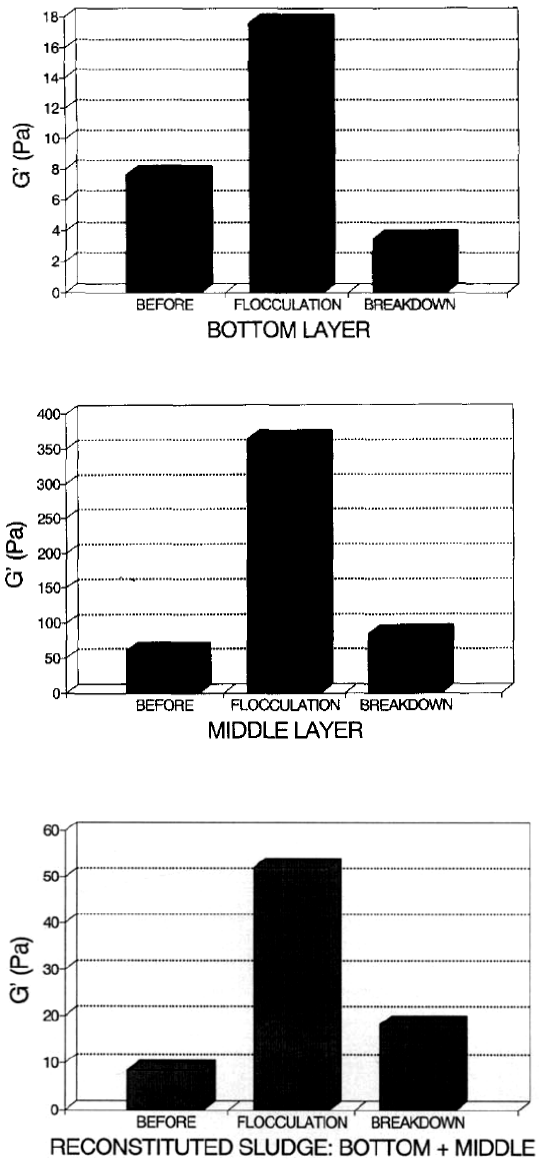

Figure 2-22 Elastic modulus of the bottom and middle layers and reconstituted sludge before shearing, after flocculation and after deflocculation [39]

Elasticity ($G^{'}$) of the middle layer sludge is the highest among the three cases. The bottom layer shows minimum amount of elasticity while the elastic modulus of reconstituted sludge lies between the values of middle and bottom layer. Another interesting point is the relative value of $G^{'}$ before shearing and after deflocculation due to excessive mixing. Figure 2-22 shows that for the case of middle and reconstituted layers the elasticity of the sludge after floc breakage by excessive shearing is higher than the original sample, whereas in the case of bottom sludge the elasticity becomes lower after excessive shearing. Thus, it seems that the middle layer forms stronger aggregates. Angle et al. suggested that this is attributed to the hydrophobic bonding which is predominant in the middle layer due to the presence of higher organic content.

3 Experimental

3.1 Materials

Mature fine tailing samples were obtained from Syncrude Canada and Suncor as the material source for experiments. MFT samples from Syncrude were taken from Mildred Lake Settling Basin (MLSB) and West In Pit (WIP) ponds.

Chemicals such as ferric sulfate, sodium hexametaphosphate (Calgon), manganese chloride, and Magnofloc 1011 (anionic polyacrylamide flocculant), used in different stages of experiments were obtained from Fischer Scientific.

For dilution of the samples and for polymer solution preparation, deionized water with conductivity of 15 MΩcm was used.

3.2 Equipments

3.2.1 Beaker, baffles and impeller

For the case of mixing the slurries, the goal is to find an optimum configuration and mixing rate. Any geometrical configuration might be criticized as not being the optimum one. However, for this project a standard geometrical configuration of beaker and baffle described in Figure 3-1 was used [40].

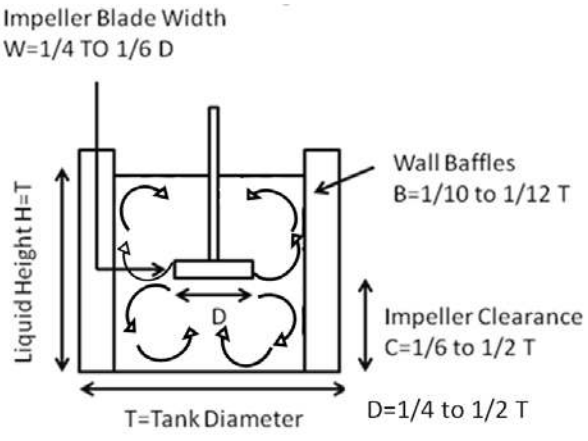

Figure 3-1 Mixing geometrical configuration [40]

The curved arrows in this figure show the pattern of mixing in the beaker. A Rushton turbine impeller was used in the designed mixing beaker. The geometrical configurations of the mixing beaker are presented below:

T= 7.5 cm

C= 2.5 cm

B= 0.6 cm

D= 3.5 cm

W= 0.7 cm

3.2.2 Rheometer

Rheological behaviour of samples was measured by the ARG2 rheometer from TA instrument. Due to the settling of the particles especially where the samples were flocculated as the result of polymer addition, Vane rotor geometry was used. Figure 3-2 shows such a geometry which keeps the particles suspended during the measurements. Other types of geometries such as cone and plate, concentric cylinder or parallel plate were not suitable for the samples in which settling occurs, as they may measure only the supernatant rheological properties.

Figure 3-2 Vane rotor (left) and cup (right) used for rheology measurement

For gelation rate tests, viscosity measurements and viscoelasticity measurements, suspensions of 10 wt% fine particles were prepared by adding 10 g of desired fine solids to 90 g of Syncrude process water and mixing the resulting slurry at 1460 rpm for 25 minutes. For these tests the temperature was set to 25°C in the conditioning and post experiment steps. For gelation rate measurement, time sweep test was conducted over 30 minutes with oscillatory stress of 0.001 (Pa) and angular frequency of 0.3926 (rad/s). For viscosity measurements steady state flow tests was performed in shear rate range of 0.1 (1/s) to 10 (1/s). For viscoelasticity measurements strain sweep test was conducted in strain range of 0.0001 (%) to 0.1 (%) (which is the linear viscoelastic range for the prepared suspensions) with angular frequency of 3.14 (rad/s).

3.2.3 Particle size analyzer

To measure the particle size distribution in different MFT samples, samples were taken from different locations while getting mixed in the beaker and baffle system described in Figure 3-1. For the cases where samples were flocculated, sonication and dispersing of the particles were implemented prior to particle size analysis. Sodium hexametaphosphate (Calgon) was used in these situations. The particle size distribution (PSD) of the samples then was measured using Malvern Mastersizer 2000 which uses the laser diffraction principles. Particles passing through the laser beam will scatter the light. The angle and intensity of the scattered light is related to the size of the particles. Smaller particles scatter the light of lower intensity at wider angle whereas larger particles scatter the light of higher intensity at narrower angle. Transmission of light also occurs, which is taken into account by implementing the refractive index in the measurements [41]. Illite was chosen as the reference for the refractive index of the MFT samples as it is one of the most abundant clay minerals in MFT.

3.2.4 Thermal analyzer

STA 409 PC Luxx thermal analyzer from Netzsch Instrument was used for thermogravimetric analysis of the samples. This apparatus is equipped with a top loading balance with capacity of 18 g and can heat the sample up to 1550°C. Desired solid particles, which were dried in vacuum for 48 hours were grinded by mortar and pestle for TGA, XRD and FTIR tests. For TGA tests first the base line was measured. In order to construct the base line two empty crucibles of 158 mg weight were put on the loading balance. The temperature was set to increase from 30°C to 900°C during 1 hour and 26 minutes and stayed constant for 30 minutes after that. This base line was used for the TGA tests. 10 mg of the desired sample was put into one of the crucibles and together with the other empty crucible was placed on the loading balance. The temperature was increased in the same manner mentioned above and the weight loss percentage of the sample was measured.

3.2.5 Plasma asher

In order to study the properties of the clays, the organic fractions on their surface need to be removed. One may seek a procedure which does not alter the phases of the clays. Plasma ashing is a proper method in this case as the combustion happens at low temperature. A K1050X plasma asher was used for the removal of organic content from clays. This apparatus consists of a reaction chamber, a vacuum pump and a radio frequency (RF) generator. The RF generator provides up to 150 watts of radiation power of 13.56 MHz continuous wave to the reaction chamber. The vacuum pump is interlocked with the RF generator switch to prevent RF power to turn on before reaching the desired vacuum level.

The sample is loaded in to the reaction chamber. The carrier gas molecules introduced to the chamber are excited by the RF power applied around the chamber and get dissociated into chemically active atoms. The combustion products are carried away by the gas stream. In this project organic materials in

the solids were removed via 10 cycles of ashing with a power of 50 watts and duration of 30 minutes whenever it was needed.

3.2.6 Fourier transform infrared spectrometer (FTIR)

BioRad FTS6000 was used for acquiring infrared spectra. A schematic figure describing working principles of FTIR is shown in Figure 3-3.

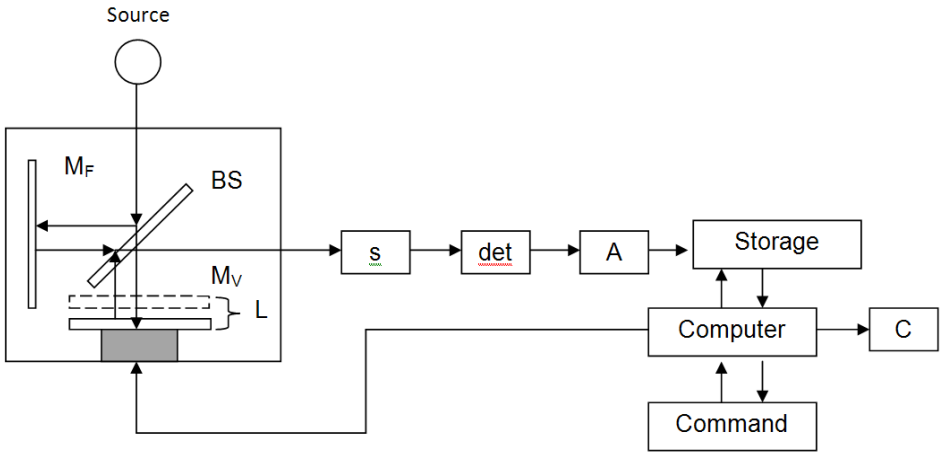

Figure 3-3 FTIR instrument block diagram

This instrument is able to record infrared spectra of solids and gases in the range of 400 to 1100 cm^{-1}. As shown in Figure 3-3, the source emits the beam including all infrared frequencies to a beam splitter, BS. Beam splitter divides the beam into two parts as it reflects half of that to a fixed mirror M_F and transmits the other half to a moving mirror M_V. These two beams are recombined at BS where the beam reflected from the M_V has traveled a longer distance equal to L, which is variable. The recombined beams at BS in turn are sent to the sample S. After transmission through the sample the radiation is converted to an electric signal in the detector, processed in A and then recorded by the computer. The resultant spectrum is in the form of percent transmission as a function of wavenumber [42].

Prior to use the FTIR instrument, the detector was cooled down with two full funnel of liquid nitrogen for about 20 minutes. Potassium bromide (KBr) was used as the reference in FTIR test. For background measurement the FTIR

spectrum of pure KBr was measured. The background spectrum was checked to make sure that no water (detectable by the peak at 1000 cm^{-1}) or CO_2 (detectable by the peak at 1600 cm^{-1}) exist in the KBr. In order to prepare the samples about 0.1 g of KBr was mixed and grind with 1-5 mg of the desired sample for 2-3 minutes in a mini pestle. The sample was put in the sample holder and pushed in the machine for measurement. The purge opening was closed during measurements and open for a few minutes after changing the samples to make sure that no air exists in the detector during measurements.

3.2.7 Zeta potential

Brookhaven ZetaPALS was used for the zeta potential measurement of the samples. The apparatus is designed to measure the zeta potential of suspensions or macromolecules within the range of 10 nm to 30 μm. Applying an electric field to a liquid suspension where particles are charged will cause the particles to move towards negative or positive poles depending on the sign of their charges. The velocity at which they move depends on the magnitude of their charges. Two laser beams, one as the reference, with frequency difference of ω_S cross the interface region where particles mobility is measured. A particle fixed in a position scatters light with a fixed phase shift relative to the reference signal while moving particles will cause a time dependent phase shift of the scattered light, which is used for the calculation of the mobility and zeta potential of the particles. The governing equation for this calculation is:

$$\mu = \xi \frac{\varepsilon}{\eta} f(ka) \qquad \text{Eq 3.1}$$

in which μ is the electrophoretic mobility, η is the viscosity, ε is the dielectric constant and ξ is the zeta potential of the particle. ka is the ratio of particle radius to double layer thickness. $f(ka)$ is called Henry's function and it is unity for large ka.

The Brookhaven ZetaPALS instrument was turned on 30 minutes before the measurements. The cuvette used for the measurements was filled to 1/3 of its volume. The electrode was put into to the cuvette and it was checked that no bubble exists on the electrode or cuvette wall. The cuvette was put in the measuring slot. The measurement parameters such as pH and number of runs were then set and the tests were conducted.

3.2.8 X-ray diffractometer (XRD)

Identification of different types of minerals in clays was done using Rigaku Rotaflex X-ray diffractometer. X-ray diffraction technique is based on the Bragg's equation:

$$2d \sin\theta = n\lambda \qquad \text{Eq 3.2}$$

where d = distance between planes of crystals

θ = angle at which an incident X-Ray beam hits the sample

λ = wavelength of the incident (source) X-Ray beam

Figure 3-4 shows the working principles of an XRD instrument.

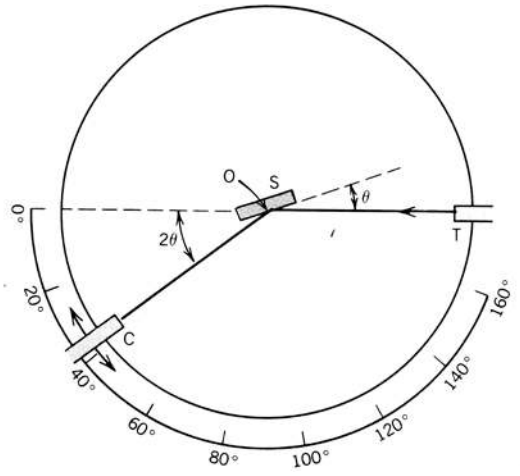

Figure 3-4 Schematic diagram of an X-ray diffractometer

In this figure, T is the X-Ray source, S is the sample, C is the detector and O is the axis around which the sample and detector rotate, and 2θ is the diffraction angle.

The X-ray source used for XRD could be produced by a "Fixed tube" also known as fixed anode or by rotating anode. In the first case the anode is fixed in a tube under vacuum and X-Ray is generated when electrons with sufficient energy strikes the anode. In rotating anode mode, anode rotates with high speed and X-Ray is generated when electrons from fixed cathode strikes the anode. The anode in both cases could be either cobalt or cupper.

Results produced from the XRD are in the form of intensity of the diffracted beam versus diffraction angle (2θ). The corresponding values of the peaks then are converted to the d (the characteristic parameter of crystalline plates) and are compared with standard samples XRD patterns [43].

For XRD tests in this work, the area of 1/2″×1/2″ of a glass slide with dimension of 3″×1″ was smeared with vaseline. The sample powder then was sprinkled on the vaseline and pressed with another blank glass slide to stick to it. The bottom half of the glass was then inserted into the horizontal goniometer and the sample was scanned by the incident X-ray beam hit from 10 degrees to 110 degrees at the scan speed of 2 degrees per minute.

3.3 Fine particles separation

Two types of fine particles were separated from MFT sample (provided from Syncrude WIP pond) with a physical fractionation method for further characterization in this project. The procedure of the fractionation is illustrated in Figure 3-5. 50 ml of MFT was diluted with 150 ml deionized water. The resulted slurry was left to settle for two days. The coarse particles in the slurry settled after two days and the suspension of the fine particles on top of the coarse sediment was separated with a pipette. The separated suspension was sieved to obtain the suspension of fine particles of sizes smaller than 28 μm. For this purpose wet

screening method was applied, using sieves with size of 75 µm, 45 µm and 28 µm. The sieves with size of 75 µm and 45 µm were only used to separate coarse particles which could block the 28 µm sieve. The undersize fraction of 28 µm sieve was then centrifuged at 2300 rpm, which resulted in formation of two layers of solids: one as light color sediment in the bottom of the centrifuge tube and another on top of the sediment with dark color. The dark suspension was separated from the light sediment using a pipette. The separated fine particles were washed twice with Syncrude process water with water chemistry shown in Table 3-1. This water has a similar chemistry to MFT water from WIP pond (shown in Table 3-2). The purpose of using process water as washing water was to make sure that the surface properties of clays were preserved after dilution. The washed clays were then centrifuged at high rpm (12000 rpm) and put aside for characterization tests. In this work whenever the terms light and dark fine particles are used they refer to particles fractionated by the method described above. The dried solids of the separated fractions and their particle size distributions are shown in Figure 3-6.

Table 3-1 Syncrude process water chemistry

Syncrude process water	
pH	8.4
Ca	14.1ppm
Mg	16.6 ppm
Mn	<0.05 ppm
Fe	<0.05 ppm
Na	575 ppm
K	20.7 ppm

Table 3-2 Water chemistry of MFT from WIP pond

Syncrude MFT (WIP)	
pH	7.82
Ca	15.2 ppm
Mg	9.2 ppm
Mn	0.06 ppm
Fe	0.10 ppm
Na	654 ppm
K	13.7 ppm

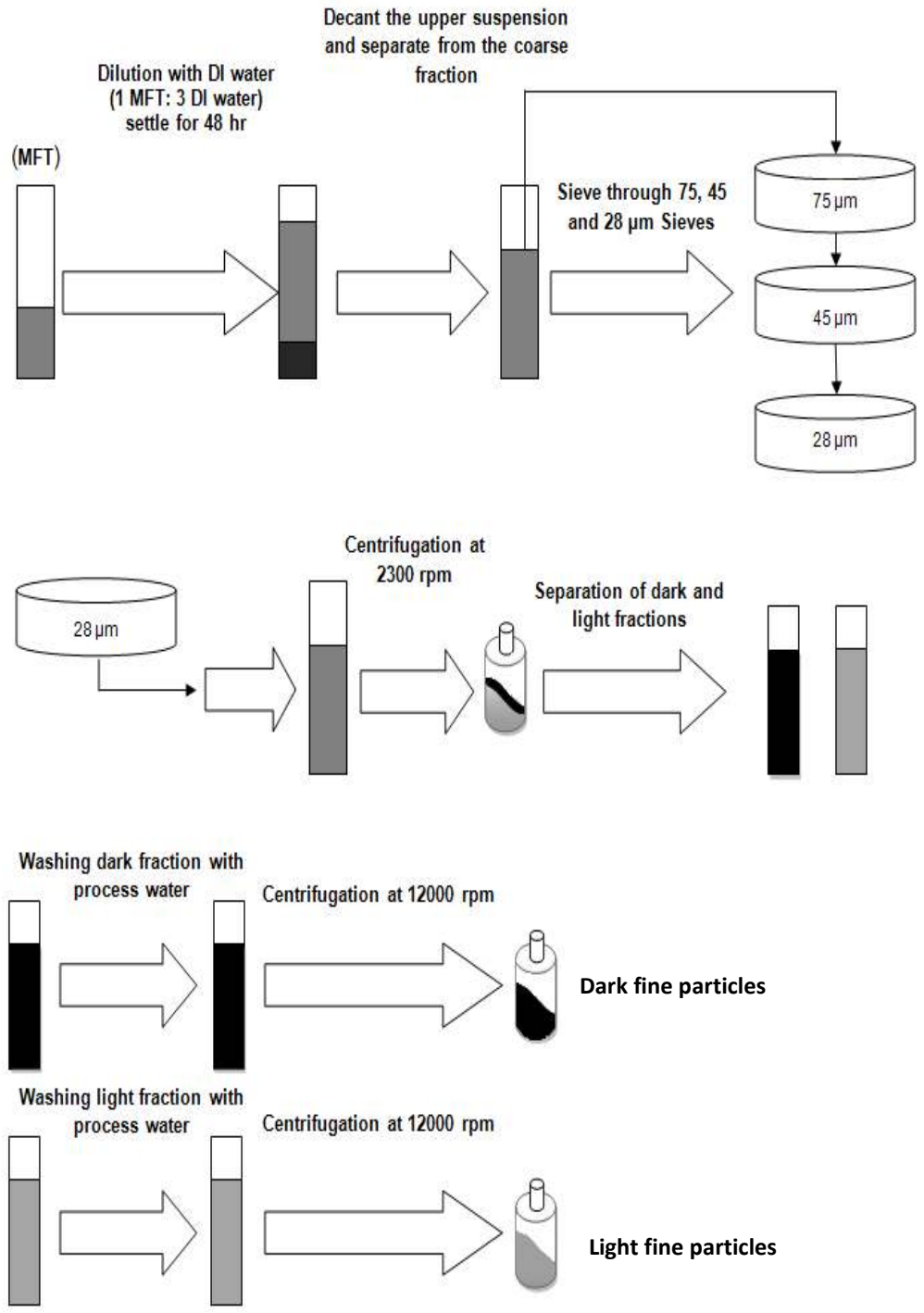

Figure 3-5 Schematic diagram of fractionation of fine particles from Syncrude WIP MFT

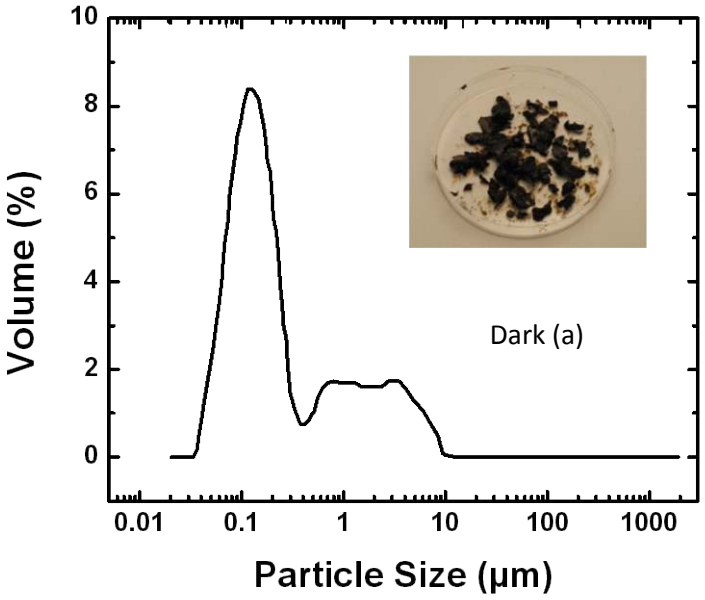
Volume (%)
Particle Size (μm)
Dark (a)

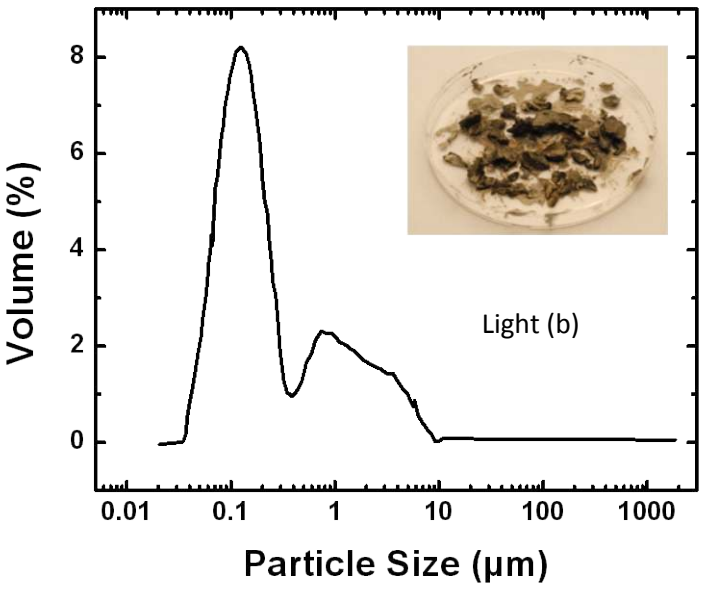
Volume (%)
Particle Size (μm)
Light (b)

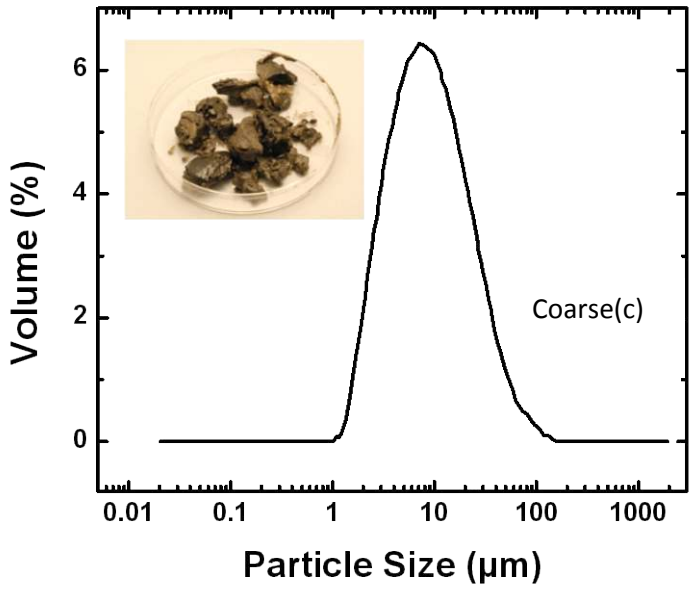

Figure 3-6 **Fractionated (a) dark fine, (b) light fine and (c) coarse particles, and corresponding particle size distribution (fractionated from Syncrude WIP MFT)**

4 Effect of water chemistry and dilution on solid sedimentation and flocculation

In this Chapter the effect of changes in water chemistry and dilution of MFT on solid sedimentation and flocculation is investigated. In the first section, settling of solid particles after flocculation by Magnofloc 1011 for two different MFT samples from Suncor and Syncrude is investigated. The results show that a better sedimentation of the Suncor MFT might be due to presence of iron cations in this sample. In the next step the effect of addition of iron cations on settling of the solids in Syncrude MFT is studied. The results show that addition of iron cations improves the sedimentation of solids in Syncrude MFT.

In the second section of this Chapter the effect of dilution on sediment solid concentration and initial settling rate of the particles is analyzed. Except for the first section of this Chapter (Section 4.1.1), MFT sample from Syncrude MLSB pond with the water chemistry shown in Table 4-1 was used for the results presented.

Table 4-1 Water chemistry of MFT from MLSB pond

Syncrude MFT (MLSB)	
pH	7.9
Ca	15.1 ppm
Mg	10.3 ppm
Mn	<0.05 ppm
Fe	<0.05 ppm
Na	1075 ppm
K	13.2 ppm

4.1 Effect of water chemistry on solid sedimentation

4.1.1 Settling of the solid particles from Suncor and Syncrude MFT

Water chemistry is an important factor in flocculation of solid particles as it has a significant effect on attractive and repulsive forces between solids. Ion chromatography (IC) was used for measuring the concentration of several ions in the water of two MFT samples from Syncrude and Suncor. The results of these tests are shown in Figure 4-1, Figure 4-2 and Table 4-2. Due to caustic addition during the extraction process, concentration of sodium ion in both cases was considerably high. Calcium and magnesium concentrations were similar in both samples and potassium content in Syncrude sample was slightly higher. An interesting observation was the difference in the color of water samples, after centrifugation of whole slurries for half hour at 12000 rpm. Water sample from Suncor's MFT appeared to be yellow, possibly due to the presence of iron cations in the water.

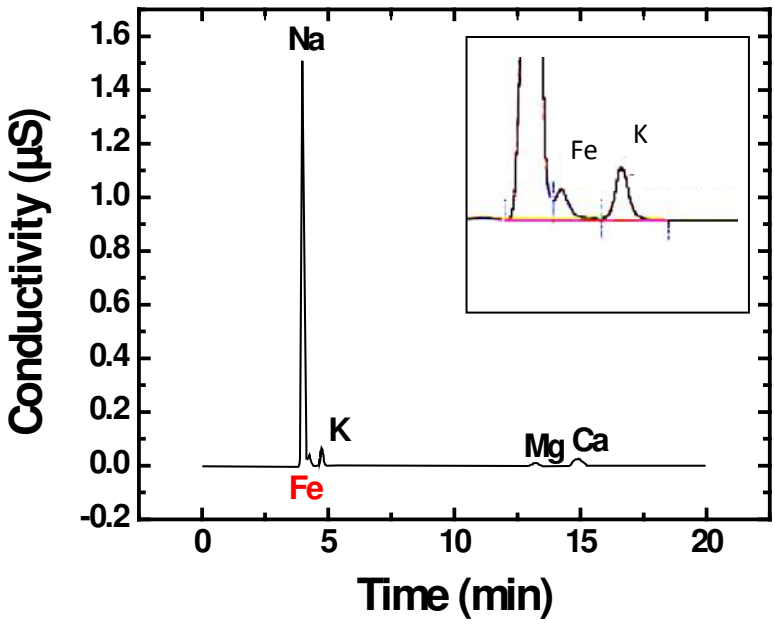

Figure 4-1 Ion chromatography results of Suncor MFT water

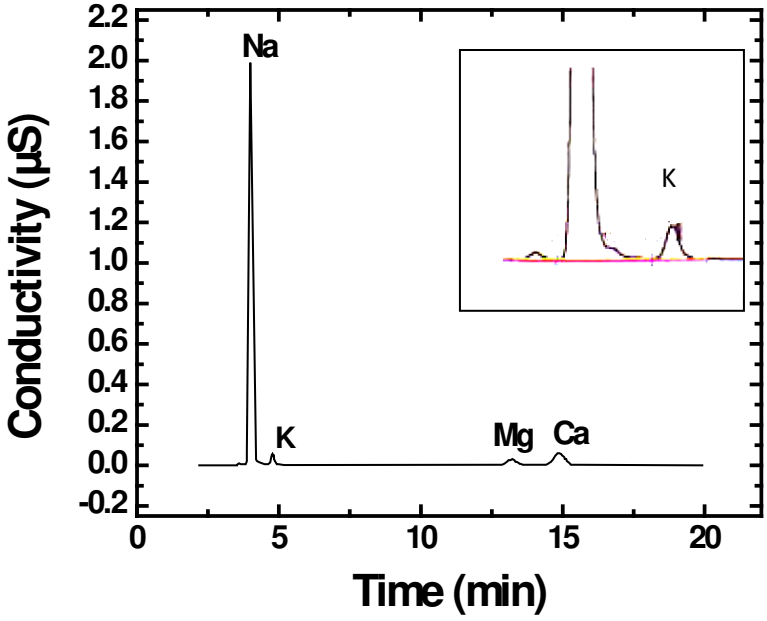

Figure 4-2 Ion chromatography results of Syncrude MFT water

Table 4-2 Syncrude and Suncor MFT water chemistry

	Syncrude	Suncor
Solid content (wt %)	38	32
Water chemistry (ppm)		
Ca	9	8
Mg	13	20
K	52	30
Na	806	604
Fe	Not detected	Detected

Results from the Figure 4-1 shows the presence of Fe cations in Suncor MFT water while no Fe cations was detected in Syncrude MFT water as shown in the inset of Figure 4-2. To measure the exact concentration of a specific ion, the area below the corresponding peak should be measured. As shown in the inset of Figure 4-1, the peaks of Na and Fe ion were not split completely due to the similar retention time of these ions in the chromatography column. As a result, the

area under the peak of Fe cations and hence their concentration was not measurable.

The sedimentation of the solid particles in aqueous media due to flocculation by macro molecules depends on the water chemistry and properties of solid particles.

In the next step, the size distribution of particles in these two samples was measured using Malvern Mastersizer 2000. Figure 4-3 shows the particle size distribution of these two original MFT samples before flocculation. A bimodal PSD was observed in both cases. The fraction of solids which are less than 0.5 µm is known as ultrafine solids and the fraction larger than 44 µm is known as coarse fraction. Particles with the size between these two numbers are labelled as fine fractions.

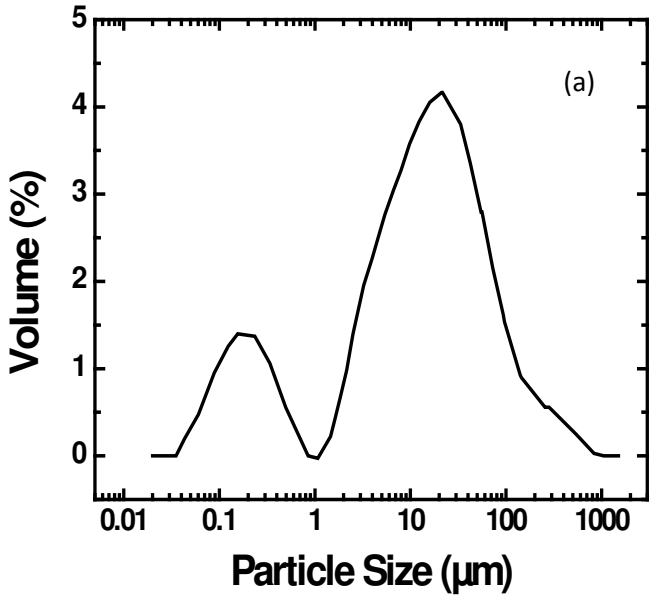

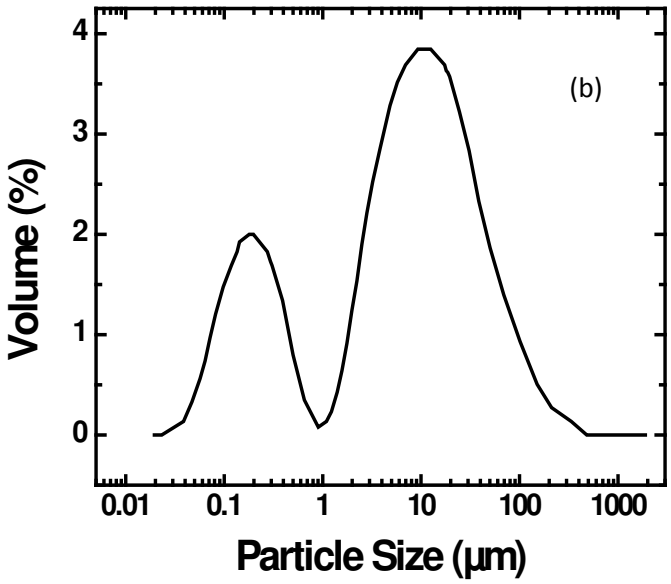

Figure 4-3 PSD of solids from (a) Suncor and (b) Syncrude MFT

The PSD of the original MFT samples in Figure 4-3 show that particles in both samples are of similar size distribution. X-ray diffraction analysis was conducted to determine the difference in the type of minerals in these two MFT samples. The XRD patterns of solids from these two MFT samples, shown in Figure 4-4, are almost identical, suggesting the same types of minerals.

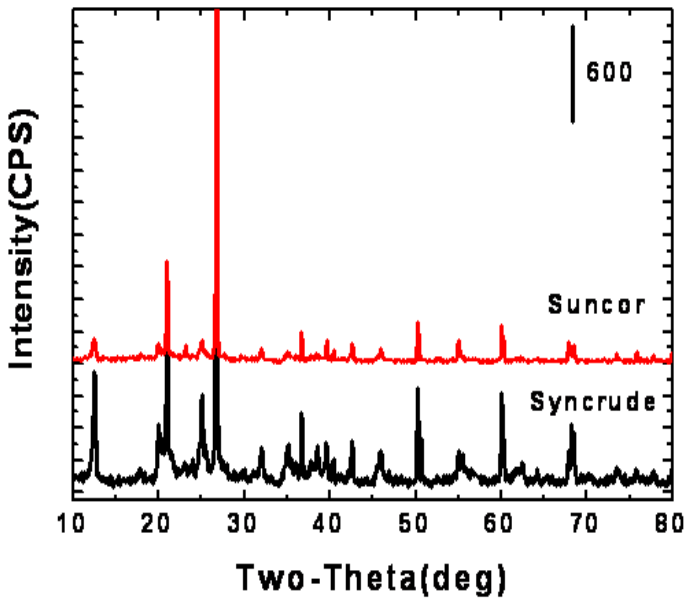

Figure 4-4 XRD pattern of solids from Suncor and Syncrude MFT

To observe the sedimentation behaviour of solids in suspension of different water chemistries a comparison was made between these two MFT samples of original solid concentration of 38 wt% and 32 wt% from Syncrude and Suncor, respectively. To make sure that all particles are dispersed, 100 ml of each sample was premixed at 1000 rpm in the mixing beaker for 5 minutes. Magnofloc solution was then added to the slurries over 90 seconds while they were mixed at 350-370 rpm to adjust the polymer concentration to 250 ppm (regarding the solids) in both samples. The flocculated slurries were then poured into a graduated cylinder through a funnel and the particle settling rates (mud line location) were observed. The observations showed no settling of Syncrude MFT samples, which resulted in no release of water, even after a day. There was a slow settling in Suncor MFT sample leading to a portion of clear water on the top of the sample after half hour sedimentation. It is important to note that no water was released in both samples without polymer addition even after mixing.

According to Stokes' law (Equation 4.1), the size (d_p) and density (ρ_p) of solids have direct effect on particles settling velocity.

$$V_S = \frac{(\rho_p - \rho_f) g d_p^{\,2}}{18 \mu_f} \qquad \text{Eq 4.1}$$

As mentioned before, it seems that there is no significant difference in the size and types of mineral solids in these two MFT samples. The same XRD patterns shown in Figure 4-4 also suggest the same density of particles (ρ_p). Thus the difference in the settling of these two samples might be related to the difference in water chemistry. Changing the water chemistry causes changes in the sedimentation behaviour of the solids by changing apparent particle sizes of aggregates. As mentioned before, the difference in the iron ion concentration was observed between the two MFT samples. It seems that changing the iron ion concentration can affect the flocculation and sedimentation of the particles. To observe this effect, a comparison was made on Syncrude MFT sample, with and without iron concentration adjustment. $Fe_2(SO_4)_3$ was used to adjust the Fe concentration in the slurry. In the case of no iron adjustment, 40 ml of the slurry was taken and premixed at 1000 rpm for 5 minutes. 40 ml of 200 ppm polymer solution was added to the slurry while mixing at 350-370 rpm for 90 seconds. Concentration of polymer in the resulting slurry was 401 ppm regarding the solids in this case. The slurry was then poured immediately into a graduated cylinder and sedimentation was followed for 2 hours. In the second case, where iron concentration was adjusted, 40 ml of slurry was premixed in the same way. Followed by the addition of 16 ml polymer solution of 500 ppm polymer concentration with the same mixing procedure as in the previous case, 24 ml of 1000 ppm $Fe_2(SO_4)_3$ solution was then added to the system and mixed for 1 minute. Concentrations of polymer and $Fe_2(SO_4)_3$ were 401 ppm and 1205 ppm regarding the solids in the resulting slurry. Figure 4-5 shows the difference in the sedimentation of these two cases.

Figure 4-5 Sedimentation of solids from Syncrude MFT after flocculation by Magnofloc 1011 with (left) and without (right) Fe addition after 2 hours

The addition of $Fe_2(SO_4)_3$ results in sedimentation of solids, while no visible sedimentation occurs in the sample without iron ion adjustment. This finding explains the better sedimentation of solids from Suncor MFT by flocculation in comparison with Syncrude MFT. Thus as opposed to the hypotheses that introduce iron as a tailing stabilizer [9, 13], iron ions help the formation of flocs by flocculant addition with larger d_p and higher settling rate. Section 4.1.2 reveals the mechanism of better sedimentation of solids in Syncrude MFT by adding a coagulant ($Fe_2(SO_4)_3$) after flocculation by polymer flocculant. One should note that although the sedimentation is improved by flocculant-assisted coagulation, the amount of clear water released is not significant.

4.1.2 Study of flocculation-coagulation (FC) method on solid sedimentation in Syncrude MLSB MFT

As mentioned in Section 2.5.1, treatment of fresh tailings by flocculation followed by a stage of coagulation (FC) significantly improves the sedimentation of solids. In this section, the effect of $MnCl_2$ addition on settling of solids in MFT sample taken from Syncrude MLSB pond after flocculation by Magnofloc 1011 is investigated. $MnCl_2$ is chosen as coagulant in these tests because of its anticipated higher specific adsorption on clay surfaces in comparison with other inorganic

coagulants including $Fe_2(SO_4)_3$. In this study the procedure described in Table 4-3 was used for flocculation of MFT samples.

Table 4-3 FC treatment procedure for MLSB MFT

Procedure	Mixing time (min)	Mixing speed (rpm)
50 ml MFT+ 115 ml DI water	5	600
5 ml (1000 ppm) Magnofloc 1011	1	300
30 ml (1000 ppm) $MnCl_2$	1	300

In this case the sample was diluted by adding DI water, flocculant and coagulant solutions. The concentrations of polymer and $MnCl_2$ were adjusted to be 271 ppm and 1600 ppm regarding the solids in the prepared slurry, respectively. The result of such a treatment after two days of sedimentation is shown in Figure 4-6.

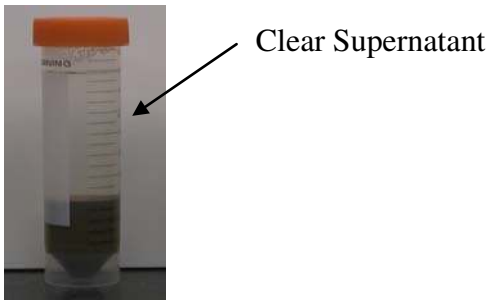

Figure 4-6 Sedimentation of solids from MLSB MFT after two days by flocculation-coagulation treatment

This experiment shows that the addition of coagulant after flocculation sweeps all fine clay particles to the bottom of settling tube. This did not happen in the case of flocculant addition alone and the supernatant was still muddy after two days as shown in Figure 4-7.

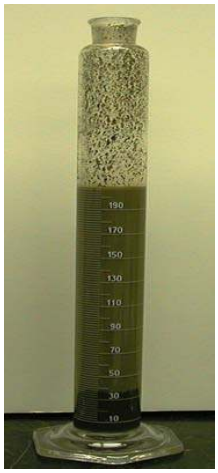

Figure 4-7 Sedimentation of solids from MLSB MFT after two days by flocculation alone treatment

As opposed to treatment of fresh tailings with FC method, which leads to recovering a considerable amount of water [35], applying FC treatment on MFT from Syncrude MLSB pond does not lead to any additional water recovery. As mentioned in Section 2.5.1, FC method improves the sedimentation of solids by attaching small aggregates to the large flocs and forming super flocs [35]. These super flocs sweep all remained fine particles to the bottom of settling tube, leaving a clean supernatant. To have a better understanding of this phenomenon, the upper suspension of the treated slurry, with flocculation only, shown in Figure 4-7 and Figure 4-8 (b), was separated after half hour sedimentation and treated with the procedure explained in Table 4-4. The treated slurry was then left for a few minutes to settle. In contrast to flocculation alone, which led to the formation of a packed sediment of coarse solids as shown in Figure 4-8 (b), the sediment solid in Figure 4-8 (a) was a network of loose super flocs.

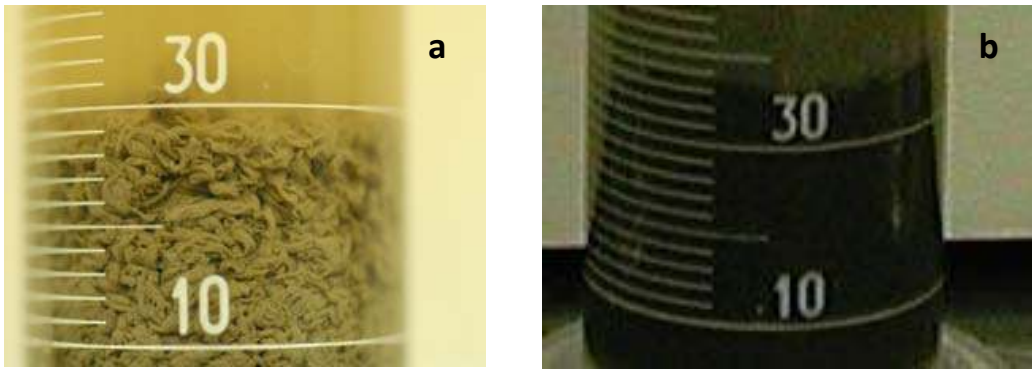

Figure 4-8 **Large and loose flocs in the sediment due to FC treatment of supernatant of b (left), small and packed flocks in the sediment due to flocculant alone treatment of the original MLSB MFT (right)**

Table 4-4 **Procedure for FC treatment of the supernatant of (b)**

Procedure for (a)	Mixing time (minute)	Mixing rate (rpm)
100 ml supernatant of b	1	600
5 ml Magnofloc 1011 of 100 ppm	1	300
30 ml $MnCl_2$ of 1000 ppm	1	300

4.1.3 Characterization of solid particles in supernatant and sediment

Different sedimentation behaviour of the particles in supernatant and sediment is also related to particle physico-chemical properties. As shown in Figure 4-7 and Figure 4-8 (b), flocculation of solid particles in MFT from MLSB pond forms two distinct layers: a layer of coarse sediment in the bottom of cylinder and a layer of fine clay suspension on the top. Below, some of the characteristics of solids in these two phases are presented.

4.1.3.1 Particle size distribution

Figure 4-9 shows the particle size distribution of particles in the sediment and supernatant after 30 minutes of sedimentation.

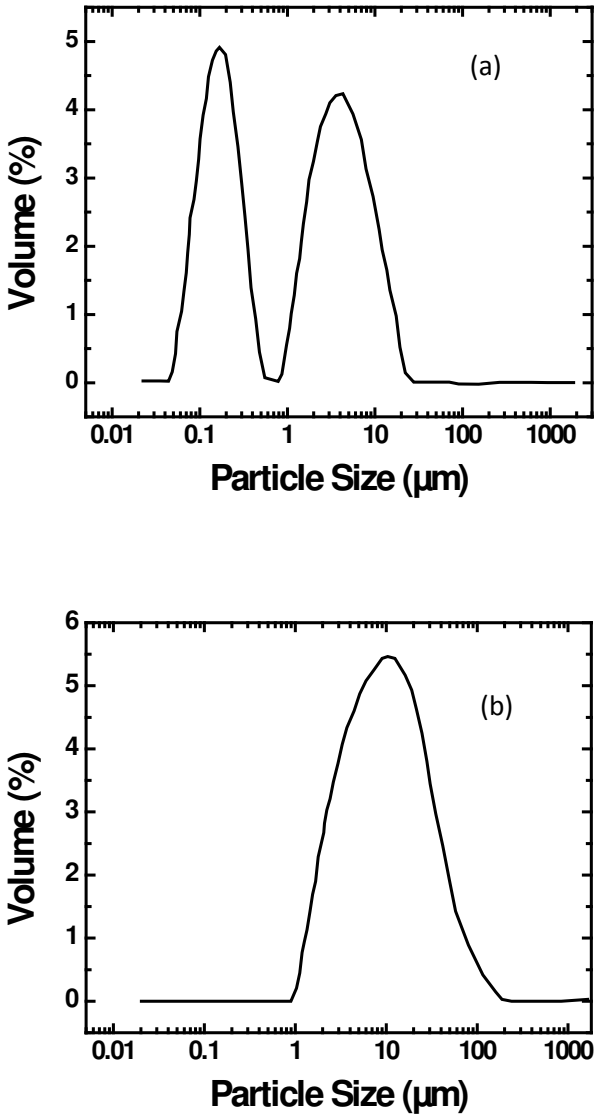

Figure 4-9 PSD of solids in (a) supernatant and (b) sediment of MLSB MFT (separated by flocculation alone treatment)

Clearly, the smaller average size of the particles in supernatant, which is less than 20 µm, keeps them suspended after 30 minutes of sedimentation, in contrast to sizes lower than 200 µm for particles in sediment. It should be noted that the fine particles with sizes between 1 to 20 µm in the sediment are those which have been swept to the bottom of the cylinder by coarse particles. However it is not clear whether size of particles is the sole key factor in their sedimentation.

4.1.3.2 FTIR analysis

Numerous chemical groups were detected for the solids from supernatant and sediment in FTIR spectra. Among the various IR peaks, those related to C-H bonds are important as the role of the organic materials on solids is an issue in studies related to MFT dewatering. Figure 4-10 shows the FTIR spectra of the solids from the sediment and the supernatant.

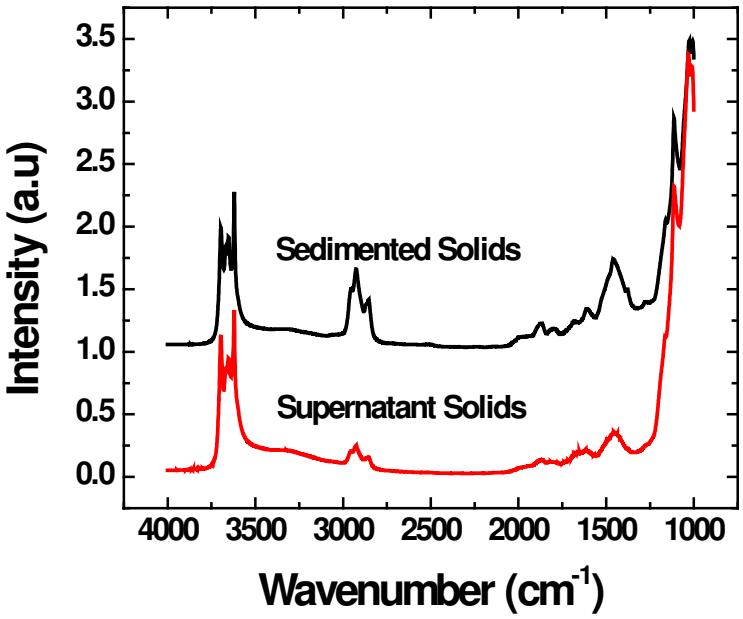

Figure 4-10 FTIR pattern of solids in supernatant and sediment of MLSB MFT (separated by flocculation alone treatment)

The results indicate that the organic content which is observable at wave number of 2900 to 3000 cm^{-1} (humic compounds) is higher for particles in the sediment. A study by Majid et al. [15] also confirmed this observation. The solids in the sediment are larger than solids in the supernatant. They also have higher organic content. It is not clear if the larger size of these particles is the only reason for their higher settling rate. The effect of organic matters on sedimentation of solids will be discussed in detail in the next Chapter where another MFT sample from WIP pond of Syncrude is analyzed.

4.1.3.3 EDX analysis

The results of EDX elemental analysis shown in Table 4-5 do not show any significant difference in the relative amounts of elements of solids in the sediment and supernatant, except for higher content of aluminum in the solids from supernatant than from sediment, which indicates the presence of higher amount of clays in supernatant phase.

Table 4-5 EDX results for solids in supernatant and sediment of MLSB MFT (separated by flocculation alone treatment)

Element	Sediment (wt %)	Suspension (wt %)
O	34.8	35.6
Na	ND	0.6
Mg	0.3	0.4
Al	5.3	13.1
Si	51.6	41.2
S	0.4	0.3
Cl	ND	0.5
K	1.9	3
Ca	1.2	0.5
Ti	0.8	0.9
Fe	3.7	3.8

4.2 Effect of polymer dosage and dilution on solid sedimentation

It has been observed that dilution helps the sedimentation of the particles [34, 35]. To better understand this effect several experiments were conducted. The results are discussed in the following section. As a basis, the effect of polymer dosage on solid sedimentation is investigated.

4.2.1 Effect of polymer dosage and dilution on sediment volume

It is well known that for a given flocculant the optimum conditions for solid settling require proper flocculant dosage and mixing conditions for treating the

sample [29, 33]. The reason for presence of such an optimum flocculant dosage is related to the mechanism of flocculation. As mentioned earlier, one of the flocculation mechanisms is polymer bridging, where macromolecules form a bridge between the particles as they attach to the particles surfaces. Increasing the polymer dosage initially improves the flocculation as it helps the flocculation of more fine particles in the slurry. After reaching a certain dosage, particle surface would be covered completely by polymer and further addition of polymer not only does not help the flocculation but also reduces the flocculation efficiency due to steric hindrance. A comparison was made on the final sediment volumes of MFT slurries of 30 wt% solids from Syncrude MLSB pond with different polymer dosages (Magnofloc 1011). The slurries were diluted by adding one volume of DI water to one volume of MFT prior to flocculation tests as no sedimentation would occur without dilution. The effect of dilution will be discussed in the next section. Diluted slurries were pre-mixed at 1000 rpm for 5 minutes and the polymer was then added to the slurry while it was under mixing at 350-370 rpm over 90 seconds. The results of these tests are presented in Figure 4-11.

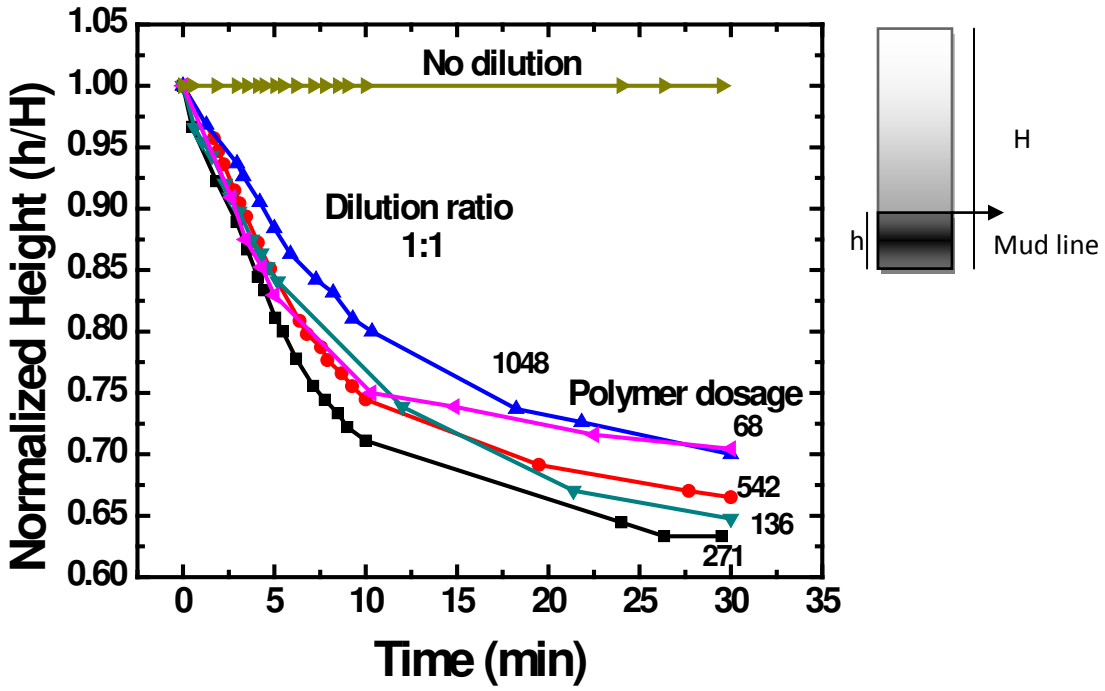

Figure 4-11 Effect of polymer (Magnofloc 1011) dosage on sediment volume (for MFT sample from MLSB pond diluted with DI water by the ratio of 1:1)

It can be observed that as the polymer dosage increases from 68 to 271 ppm (concentration of polymer regarding the solids in diluted MFT) the final height of the sediments decreases from 0.72 to less than 0.65 of its original height. Further increase in polymer dosage to 1048 ppm led to a less packed sediments, to the value of 68 ppm polymer concentration. Without dilution, regardless of the polymer dosage, sedimentation does not take place. To investigate the effect of dilution, additional tests were carried on. In these tests, for each dilution, different polymer dosages were carefully chosen and added to the slurries with the same mixing condition described on the previous page. As the slurries were diluted with deionized water, it is important to make sure that sedimentation will lead to recovery of a portion of water more than the added DI water. In order to calculate the water released in each of these conditions, fraction of water gained (FWG) defined below was used to evaluate the effect of dilution on sedimentation and water recovery:

$$FWG = \frac{V_{RW}}{V_{AW}} - 1 \qquad \text{Eq 4.2}$$

in which V_{RW} is the volume of released water and V_{AW} is the volume of added water. When $V_{RW} = V_{AW}$, $FWG = 0$, indicating zero gain of released water. A positive FWG value indicates the gain of water from original MFT and a negative FWG value indicates an overall loss of water.

Figure 4-12 shows the FWG as a function of polymer dosage at different dilution factors.

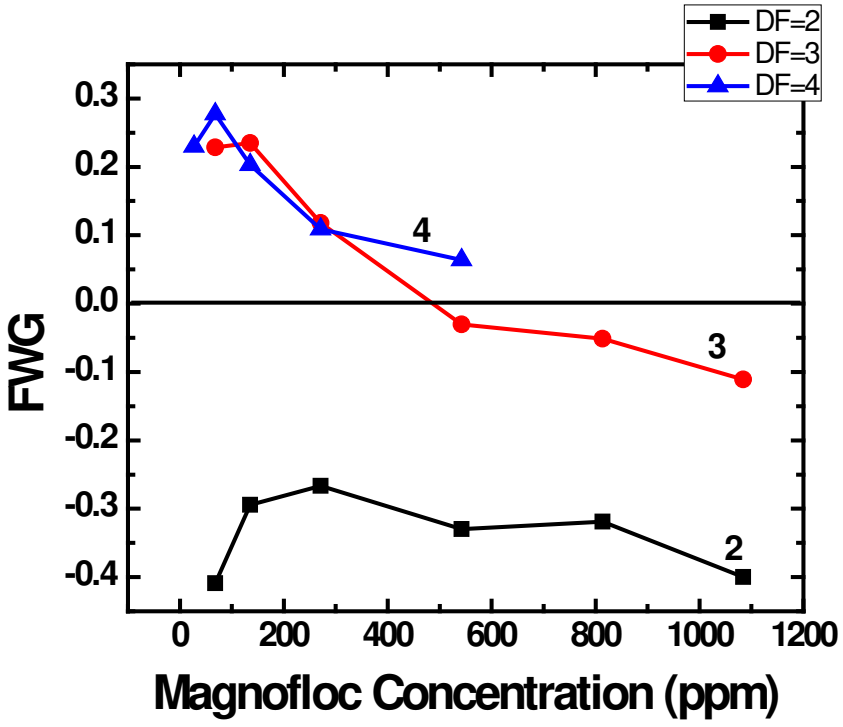

Figure 4-12 Effect of dilution and polymer (Magnofloc 1011) dosage on FWG (for MLSB MFT diluted with DI water)

In Figure 4-12 dilution factor (DF) is defined as:

$$DF = \frac{Volume\ of\ MFT + Volume\ of\ DI\ water}{Volume\ of\ MFT} \qquad \text{Eq 4.3}$$

Without dilution MFT slurry from MLSB pond of 30 wt% solid concentration did not settle by polymer addition. By diluting the MFT by DI water at a volume ratio of 1:1, i.e. a dilution factor (DF) of 2, the mud line formed and sedimentation occurred. However according to the results in Figure 4-12, the amount of released water was less than the amount of water added to the slurry for dilution, as *FWG* for all dosages of the polymer in this case was negative. At dilution factor of 3, *FWG* became positive for polymer dosage between 68 to 500 ppm. For a dilution factor of 4, *FWG* was positive up to a polymer dosage of 542 ppm, indicating overall release of water from original MFT over these polymer dosage ranges. The recovered water in all tests was still muddy after 2 days of sedimentation due to the presence of suspended fine particles as shown in Figure 4-13. Unfortunately, this gained water was not usable as the recycle water for extraction process.

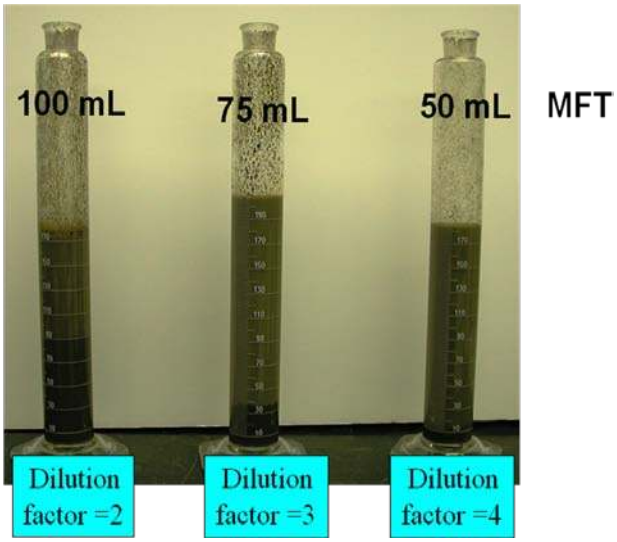

Figure 4-13 Sedimentation of solids from MLSB MFT by flocculation with polymer (Magnofloc 1011) dosage of 50 ppm for dilution factors of 2, 3 and 4 after 2 days

To observe the effect of dilution on the amount of water release, the solid content in the sediment was measured. Figure 4-14 shows the sediment solid content for the highest *FWG* at each dilution factor. Diluting the samples increases the solid

content of the sediment. This number reaches about 80 wt% by diluting the sample 4 times. It is important to note that dilution of the sample with deionized water will alter the water chemistry. Table 4-6 shows the change of water chemistry after dilution (with DI water) by a factor of four. It is interesting to note that even though the sample was diluted only four times the concentration decreased to below 1/10 of the original value for Ca and Mg ions.

Thus the increase in solid content might not be solely related to the dilution of the sample. In order to investigate the effect of dilution on sediment solid concentration without altering water chemistry, MFT should be diluted with its own water instead of DI water. For this purpose the original MFT was centrifuged at 12000 rpm for half hour and the resulted clear water from centrifuge was used for diluting the samples. The flocculation tests were repeated as described earlier in this section. The sediment solid concentrations at different dilution ratios for this case are shown in Figure 4-15. A comparison between results in Figure 4-14 and Figure 4-15 suggests that diluting MFT with its own water does not improve the sedimentation of solids as the sediment solid concentration did not exceed 26 wt% in this case.

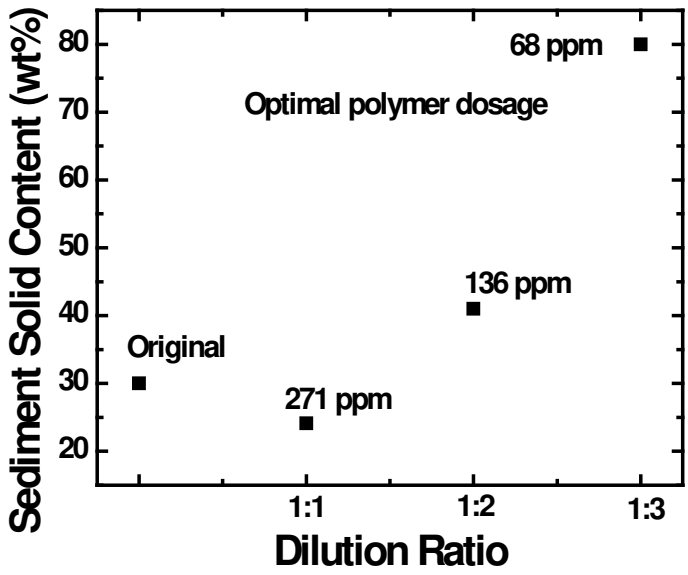

Figure 4-14 Effect of dilution (with DI water) on sediment solid concentration of MLSB MFT treated with flocculant (Magnofloc 1011)

Table 4-6 MLSB water chemistry before and after dilution with DI water with dilution ratio of 1:3 (dilution factor of 4)

	MLSB Original	MLSB Diluted 1:3
Ca	15.1 ppm	1.7 ppm
Mg	10.3 ppm	0.31ppm
Mn	<0.05 ppm	<0.05 ppm
Fe	<0.05 ppm	1 ppm
Na	1075 ppm	182.5 ppm
K	13.2 ppm	3.7 ppm

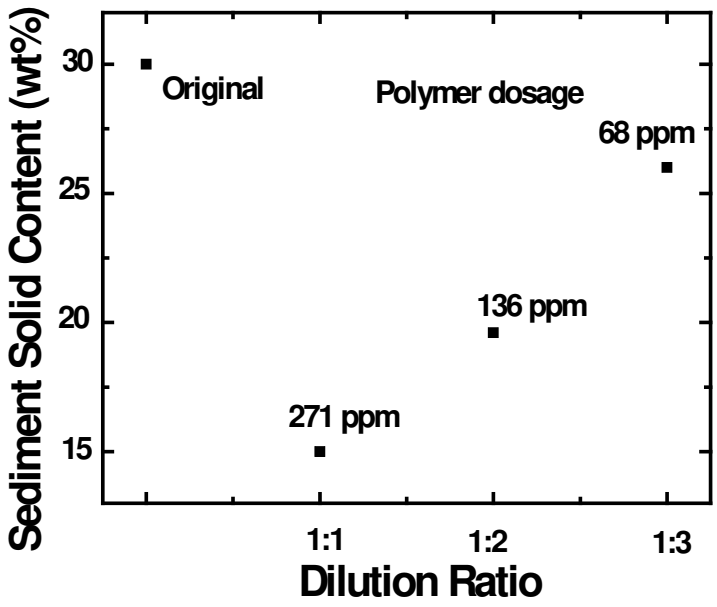

Figure 4-15 Effect of dilution (with MFT water) on sediment solid concentration of MLSB MFT treated with flocculant (Magnofloc 1011)

4.2.2 Effect of dilution on initial settling rate

Dilution also has an obvious effect on initial settling rate. Figure 4-16 illustrates this effect. Diluting the sample with DI water increased the initial settling rate. On the other hand, increasing polymer dosage decreased the initial settling rate at high dilution factors such as 3 and 4. At polymer dosages of 68 and 136 ppm (polymer concentration regarding the solids) with dilution factors greater than 3, no mud line formed and initial settling rate was not measurable.

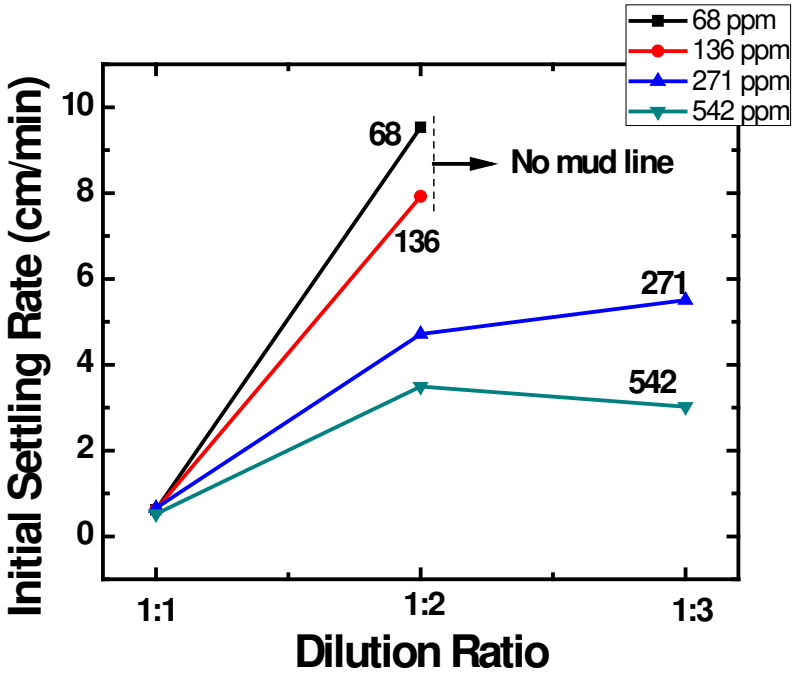

Figure 4-16 Effect of dilution (with DI water) on initial settling rate of solids from MLSB MFT at different polymer dosages

4.3 Applying flocculation treatment on another MFT sample from WIP pond of Syncrude

By adding flocculant to the MFT slurry from MLSB pond two layers were formed as shown in Figure 4-8 (b). The bottom layer in this figure was a sediment of coarse particles and the top layer was a suspension of fine particles. A brief study on the solids from these two layers in Section 4.1.3 showed that these solid particles are different in size and amount of organic matters. It is important to understand that which factor is responsible for different sedimentation behaviour in these types of solids. The answer to this question will be presented in the next Chapter where another MFT sample from WIP pond of Syncrude is analyzed.

Flocculation treatment was applied on this sample with solid concentration of 16.5 wt%. For this case, sedimentation test was done by diluting 50 ml of original slurry with its own clear water by a factor of 4 and premixing for 5 minutes at

1000 rpm followed by adding 5 ml of 1000 ppm polymer solution over 90 seconds while mixing the slurry at 350-370 rpm. The slurry was then poured immediately into a graduated cylinder through a funnel and left for sedimentation. Figure 4-17 shows the sedimentation of this sample after 48 hours.

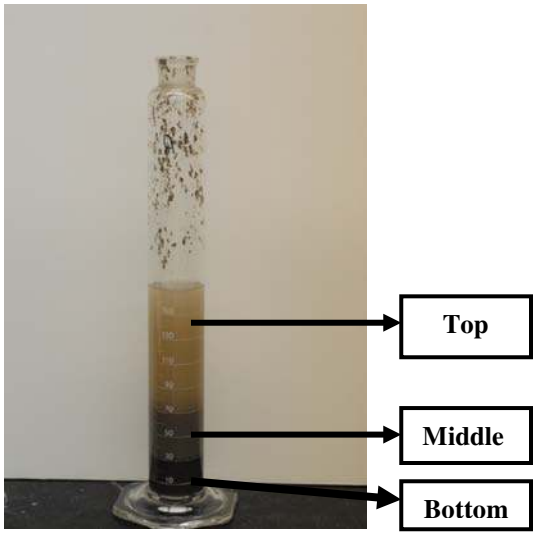

Figure 4-17 Sedimentation of solids of WIP MFT due to flocculant addition after 2 days

Three layers are easily noticeable in this figure: a packed layer of coarse particle sediment in the bottom (Bottom layer), a layer of fine particle sediment above the coarse particle sediment (Middle layer) and a suspension of fine particles in the top section of graduated cylinder (Top layer). Particle size distribution of these three layers (presented in Figure 5-1) shows that the bottom layer is a sediment of coarse particles and the top and middle layers contain fine particles with the same particle size. The same size of particles in these two layers provides us with the opportunity of studying the importance of other parameters in the sedimentation of fine particles. Next Chapter mainly deals with characterization of fine solid particles in these two layers in the context of their respond to flocculant.

4.4 Summary

In order to study the sedimentation of solid particles in MFT both liquid and solid phases should be analyzed. In this Chapter the role of water chemistry in sedimentation of solid particles was investigated. It was found that flocculation treatment alone will not result in complete sedimentation of particles. On the other hand, flocculation with Magnofloc 1011 followed by a coagulation with $MnCl_2$ (which alters the water chemistry) results in sedimentation of all coarse and fine solids. It was also noticed that diluting the samples by DI water has profound impact on settling of the particles. By simple flocculant treatment of MFT sample from Syncrude MLSB pond, coarse particles settled rapidly while fine particles stayed suspended in the water above the sediment. Applying flocculant treatment on another MFT sample from Syncrude WIP pond resulted in formation of three layers after sedimentation. Characterization of solids in these layers which is discussed in the next Chapter will enhance our understanding of stabilization of fine solids in MFT.

5 Characterizations of fine clays in the context of their response to flocculant (Magnofloc 1011) addition

In the previous Chapter, analysis of the sedimentation of diluted MFT from MLSB pond showed that adding the flocculant to the suspension changes the settling velocities of different solid particles in the diluted MFT. As discussed in Section 4.1.3 these particles were different in size, and organic content. Figure 4-9 indicated that after 30 minutes of sedimentation, fine particles with size of 0.04 to 20 µm will stay suspended in supernatant and solids with size of 1 to 200 µm settle down as packed sediment. The smaller average size of the particles in the supernatant could be the main reason for remaining in suspension. One may observe a different settling behaviour by analyzing different types of slurries such as one described in Section 4.3. In that sample (from Syncrude WIP pond) the size of solid particles is not the dominant parameter to affect the particle settling velocity. Sedimentation behaviour, solids characterization and rheological behaviour of this MFT are studied in this Chapter. These investigations reveal the importance of other parameters in sedimentation of fine particles.

5.1 Effect of size and organic content on flocculation and sedimentation of fine particles

5.1.1 Particle size distribution of top and middle layer particles and original MFT

Figure 5-1 shows particle size distribution of solids in the top and middle layers and the original MFT.

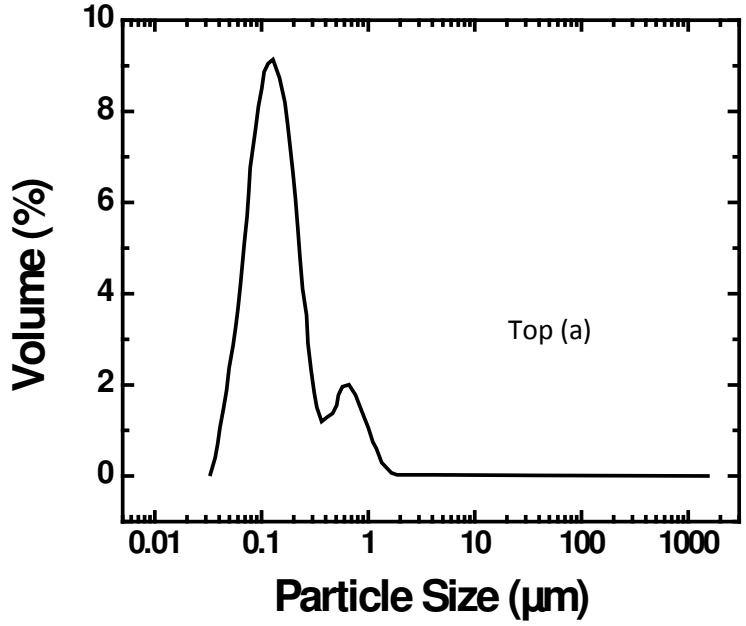
Volume (%)
Particle Size (µm)
Top (a)
0
2
4
6
8
10
0.01
0.1
1
10
100
1000

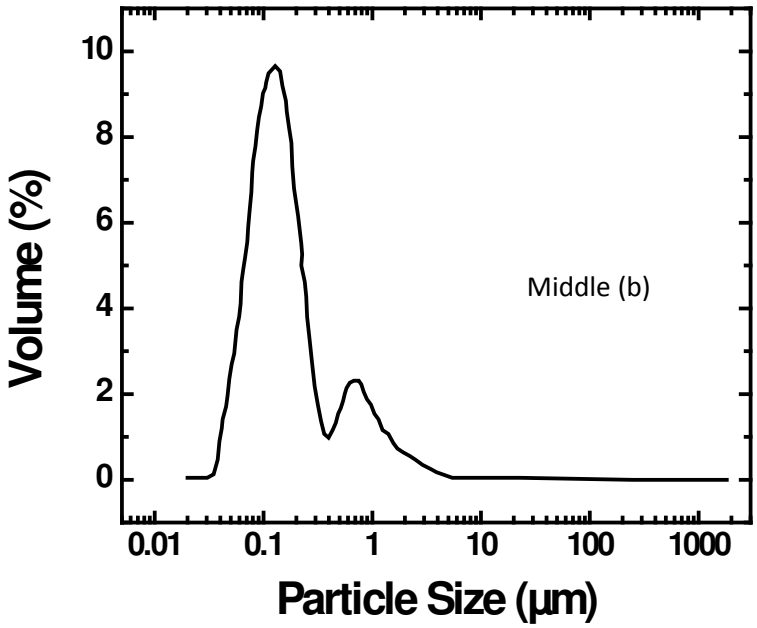
Volume (%)
Particle Size (µm)
Middle (b)
0
2
4
6
8
10
0.01
0.1
1
10
100
1000

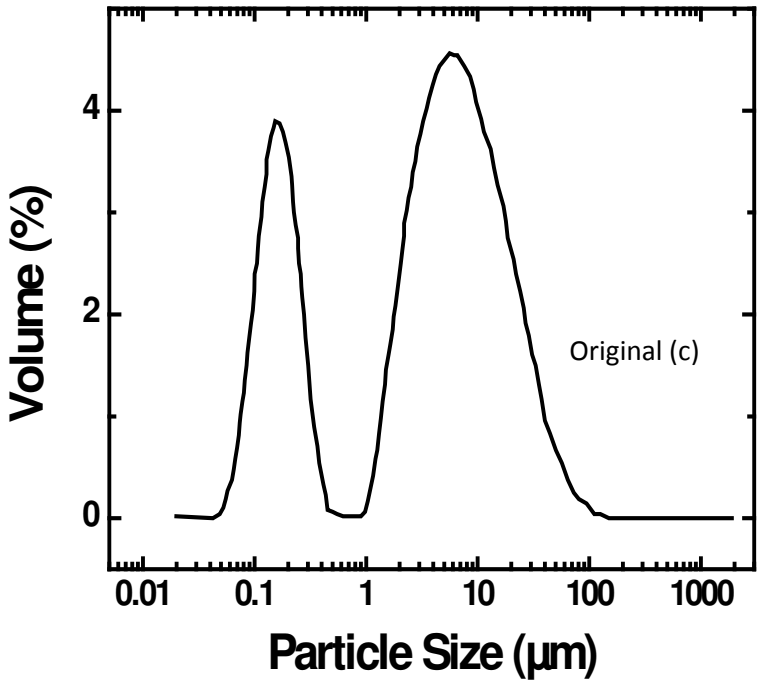

Figure 5-1 PSD of particles in the (a) top and (b) middle layers (separated by flocculant addition to WIP MFT) and (c) original WIP MFT

Figure 5-1 shows that the particles with sizes between 5 µm to 100 µm settle at the bottom of the cylinder after 48 hours. Particles in fine sediments (middle layer) have sizes between 0.03 µm to 5 µm and particles remained suspended in supernatant (top layer) are between 0.03 µm to 2 µm. The PSD in Figure 5-1 suggests that a large fraction of the particles in the middle and the top layer are ultra fine particles smaller than 0.5 µm. The cumulative PSD shows that 99% of the particles in the top and the middle layers are less than 2 µm i.e. the particles in these two layers have similar sizes. Thus particle size is not the dominant variable which governs the sedimentation in this case. Further characterization was performed to probe other properties of the solids in the top and the middle layers. It is more interesting to probe particles in these two layers, specifically the particles in the top layer, as they do not settle by polymer addition in contrast to particles in the bottom layer.

5.1.2 TGA analysis for top and middle layer particles

Thermogravimetric analysis was used to measure the amount of organic content on the solids in top and middle layers. Figure 5-2 shows the percent weight loss of the particles as a function of temperature. The temperature was increased from 30°C to 900°C at rate of 10°C /min. The solid samples were taken from the top and middle layers after 20 hours, 46 hours and 6 days of settling to investigate the change in the organic content of each phase as a function of time.

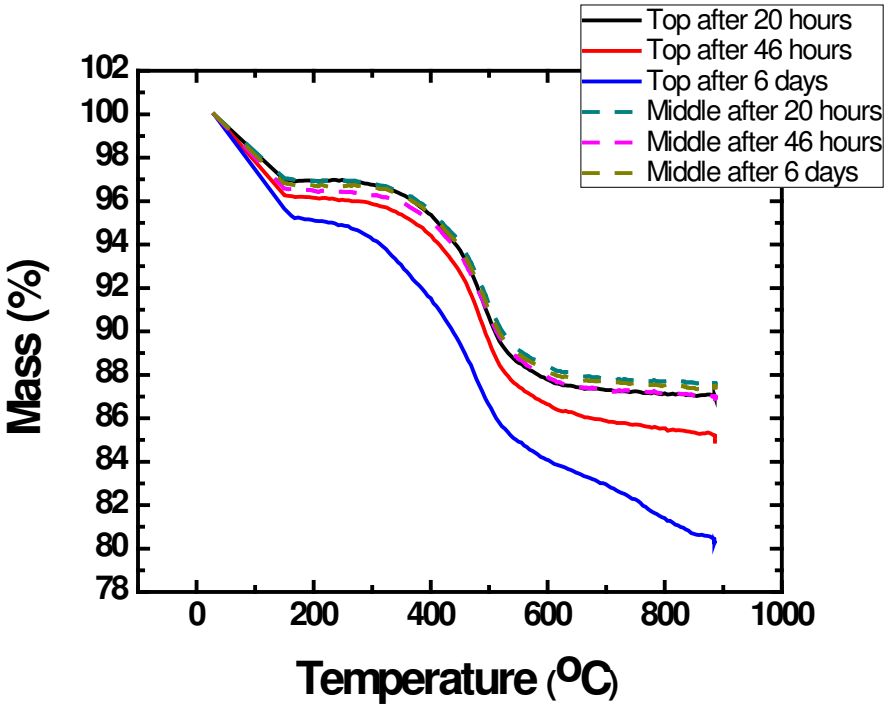

Figure 5-2 TGA analysis of solids from the top and middle layers (separated by flocculant addition to WIP MFT) after 20 hr, 46 hr and 6 days of settling

This figure shows that the amount of organic material on the solids in the top and middle layers is almost equal after 20 hr of sedimentation. On the other hand, the amount of weight loss in the top and the middle phase after 46 hours and 6 days shows that the concentration of organic content in the solids from the top layer increases with the settling time. Although the particles in the top and the middle layers have the same PSD, it appears that the difference in the organic content makes them settle at different rates. Solid particles in the top layer have slower

settling rate possibly due to their higher organic content in comparison with solids in the middle layer.

5.2 Comparisons between solid particles from the top and middle layers and physically fractionated light and dark fine particles

As mentioned in Section 4.3, by flocculant addition to the MFT slurry from Syncrude WIP pond, three different layers were formed. The solids in the top and middle layers are fine particles. The fine particles in this MFT can also be separated using the method described in Section 3.3. For this purpose physical fractionation was done by dilution, sieving and centrifugation. The resulted fractions were named light and dark fine particles according to their colours. The particle size distribution, the XRD patterns and the TGA analysis results of these two fractions and the fine solids from the top and the middle layer are compared in the following sections.

5.2.1 Comparison of the XRD patterns of light and dark fine particles with solid particles from the top layer

XRD patterns of light and dark fine particles show the presence of a variety of minerals. Background scattering is an issue which makes the interpretation of the patterns more difficult. This background scattering is supposed to occur in XRD patterns due to the presence of amorphous compounds such as those described by Majid et al. [15]. To solve this problem, particles were treated with low temperature plasma asher (LTA). Organic material in light and dark fine particles and the solids from the top layer were removed via 10 cycles of LTA with a power of 50 watt and duration of 30 minutes.

Siroquant X-ray diffraction analysis software was used for quantitative analysis of minerals in light and dark fines. These results plus the XRD patterns of the particles separated from the top suspension of the cylinder (shown in Figure 4-17) are shown in Figure 5-3. Quantitative results are also presented in Table 5-1.

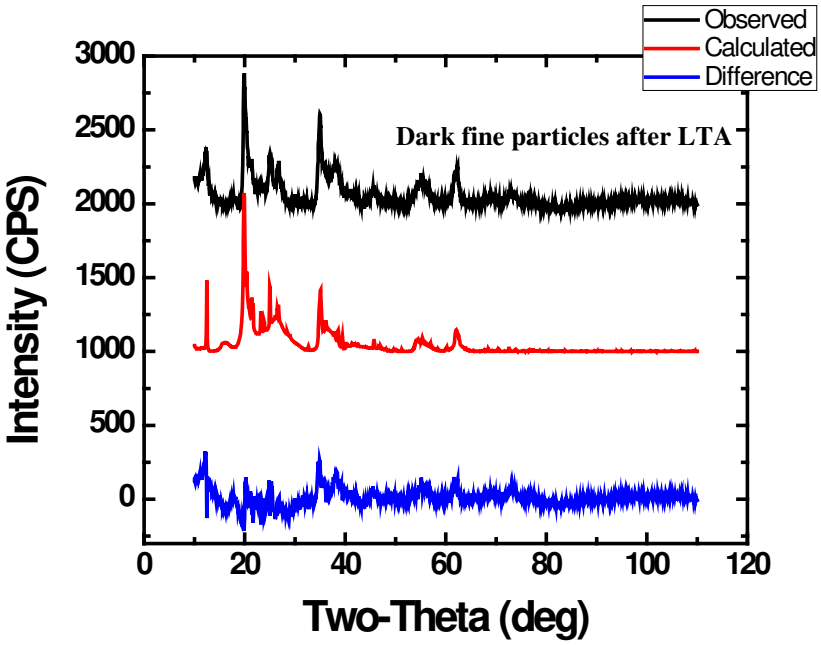
Observed
Calculated
Difference
Dark fine particles after LTA
Intensity (CPS)
Two-Theta (deg)
3000
2500
2000
1500
1000
500
0
0
20
40
60
80
100
120

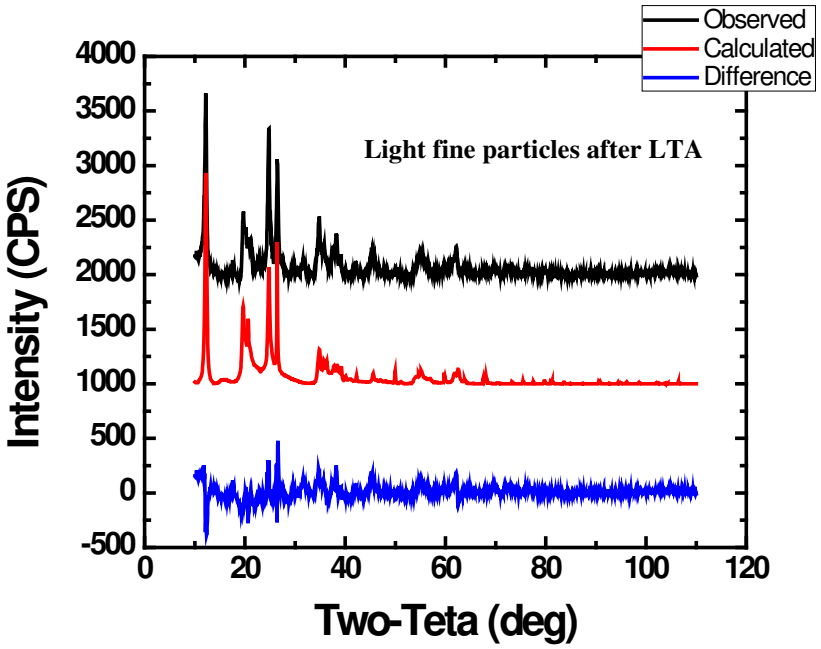
Observed
Calculated
Difference
Light fine particles after LTA
Intensity (CPS)
Two-Teta (deg)
4000
3500
3000
2500
2000
1500
1000
500
0
-500
0
20
40
60
80
100
120

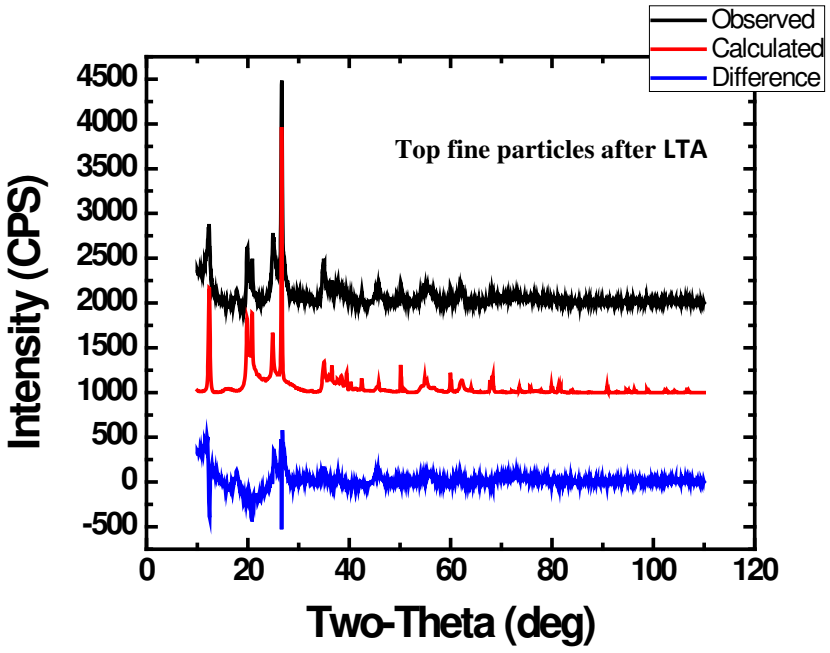

Figure 5-3 **XRD patterns for light and dark fines (fractionated from WIP MFT) and top fines (separated by flocculant addition to WIP MFT)**

Table 5-1 **Quantitative XRD (wt%) of light and dark particles (fractionated from WIP MFT) in comparison with top fines (separated by flocculant addition to WIP MFT)**

	Kaolin	Illite	Quartz
Dark fine	8.2	91.5	0.3
Light fine	37.5	56.5	6
Top fine	14.1	71.5	14.3

Figure 5-3 compares the observed diffraction patterns of light and dark fines and particles from the top layer with their associated calculated and difference patterns used to characterize the mineral types in theses fractions.

Comparing the mineral contents of light and dark fine particles in Table 5-1 suggests a higher amount of illite in the dark fine particles and higher amount of kaolinite in the light fine particles. The solids from the top layer would be mostly a mixture of the particles similar to the dark and light fine particles.

5.2.2 Comparison of the TGA analysis results of light and dark fine particles with solid particles from the top and the middle layers

Figure 5-4 shows the TGA results for light and dark fine particles. This graph indicates the presence of higher amount of organic material bounded to the dark fine particles. Comparison between Figure 5-2 and Figure 5-4 suggests that the particles in the top layer of Figure 4-17 are mostly similar to the dark fine particles as they have higher organic content in comparison with solids from the middle layer.

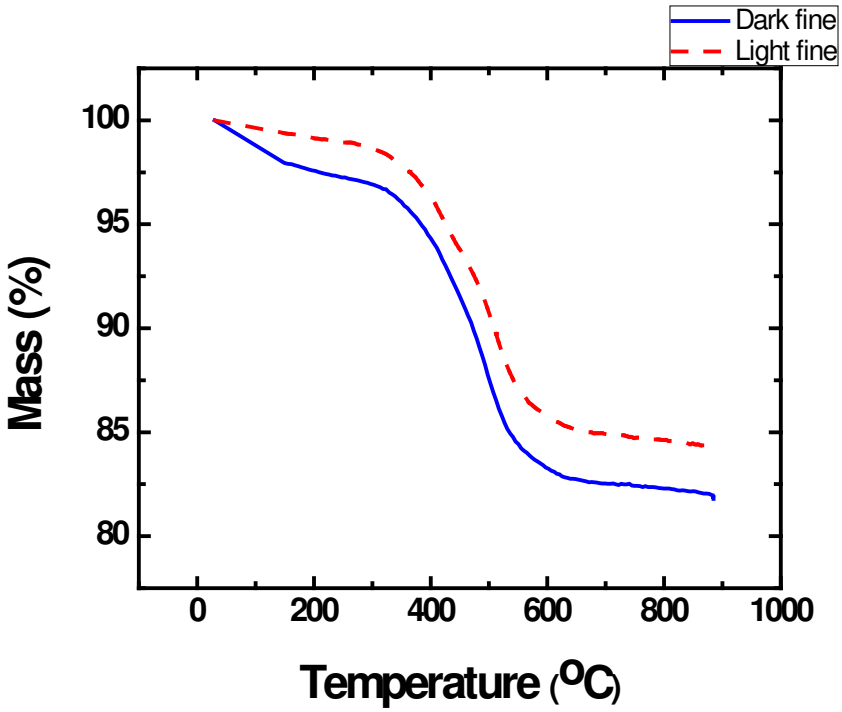

Figure 5-4 TGA analysis for light and dark fine particles fractionated from WIP MFT

5.2.3 Comparison of the particle size distribution of light and dark fine particles with solid particles from the top and middle layers

Comparison between Figure 3-6 (a) and (b) and Figure 5-1 (a) and (b) suggests that physically fractionated light and dark fine particles and solid particles from

the top and middle layer have similar sizes. All four fractions mostly consist of ultra fine particles smaller than 0.5 μm.

The comparisons made in Sections 5.2.1 to 5.2.3 suggest that the fine particles in the top and middle layer of Figure 4-17 are similar to the physically fractionated light and dark fine particles. In other words the particles in the top and middle layer of Figure 4-17 are mixtures of particles which are similar to the physically fractionated light and dark fine particles. Comparisons of the TGA analysis results described in Section 5.2.2 also suggest that the amount of particles similar to the dark fines are more in the top layer than the middle layer as the solids in the top layer have higher organic content.

As mentioned in Section 5.1.2 it seems that the slower settling rate of the solids in the top layer is due to the presence of more organic matters on these solids. Another factor to be considered is the adsorption level of flocculant on the solids in the top layer. Lower settling rate of the solids in the top layer could also be due to less adsorption of flocculant. To investigate the adsorption of flocculant (Magnofloc 1011) on the surface of fine particles, rheological tests and XPS analysis were conducted. For these tests, comparisons had to be made between solid particles without polymer (before flocculation) and with polymer (after flocculation). The solids in the top and middle layer could not be used for this purpose as they were separated from each other due to flocculation by polymer. Thus instead of using these solids, light and dark fine particles were analyzed as they were available without any flocculant on their surfaces.

5.3 Adsorption of flocculant on the light and dark fine particles

5.3.1 XPS analysis

XPS was used to investigate the amount of polymer adsorption on the dark and light fine particle surfaces. The chemical structure of Magnofloc 1011 is shown in Figure 5-5.

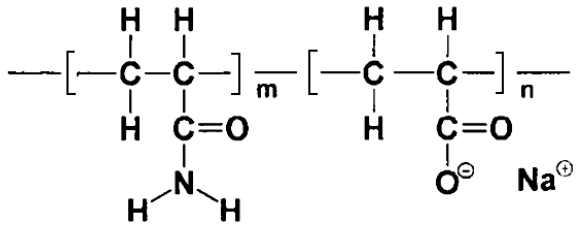

Figure 5-5 Anionic polyacrylamide –Magnofloc 1011

Magnofloc 1011 is a copolymer of acrylamide and sodium acrylate. To measure the amount of polymer adsorption on the surface of light and dark fine particles, the mass fraction of nitrogen, oxygen and carbon on the surface of the particles was measured before and after polymer adsorption. The results are shown in Table 5-2.

Table 5-2 Results of XPS analysis on polymer adsorption on light and dark fine particles fractionated from WIP MFT

Peak	Light fine solids		Dark fine solids	
Mass concentration %	Without polymer	With polymer	Without polymer	With polymer
O	71.6	60.8	83.2	82.3
N	0.4	0.8	0.6	0.6
C	28.00	38.5	16.2	17.1

As shown in the table the mass concentration of nitrogen gets doubled after the adsorption of polymer on the light fine particles but there is no change in nitrogen

concentration on the dark fine particles. Thus, it can be concluded that the level of polymer adsorption on dark fine particles is limited in comparison with light fine particles. Although this result is consistent with sedimentation test results, one might not detect the low level of polymer adsorption on the surface of dark fine particles as the maximum surface coverage of the nitrogen is less than 1 wt%, and this makes the XPS results less reliable.

5.3.2 Rheological properties of light and dark fine particles before and after polymer adsorption

In order to investigate the adsorption of polymer on surfaces of light and dark fine particles the rheological properties of these solids are discussed in their original state and after the addition of flocculant. The rheological properties of the solids from the top and middle layer (shown in Figure 4-17) are also compared with the rheological properties of light and dark fine particles to check the consistency of the results.

5.3.2.1 Viscosities of suspensions of light and dark fine particles before and after flocculant adsorption

Suspensions of 10 wt% light and dark fine particles were prepared by the method described in Section 3.2.2. Results from the Figure 5-6 show the viscosity of the suspension of dark fine particles is higher than that of the light fine particles. By adding equal amount of polymer (the polymer concentration was adjusted to be 1000 ppm regarding the solids in both suspensions) to these two suspensions, their viscosities are altered. Comparison between the results in Figure 5-6 and Figure 5-7 shows that after flocculant addition, the viscosity of suspension of the light fine particles increases considerably while no change in the viscosity of dark fine particles is detected. This finding supports the hypothesis of the lower flocculant adsorption on the surface of dark fine particles.

Suspensions of 10 wt% of solids from the top and middle layer (shown in Figure 4-17) were also prepared by the method described in Section 3.2.2. Results from the Figure 5-8 show that the suspension of solids from the middle layer has higher viscosity than that of top layer. Comparison between the results in Figure 5-7 and Figure 5-8 suggests that the solid particles from the top layer are similar to dark fine particles. This finding again supports the hypothesis that the solid particles in the top layer adsorb flocculant to a less extent.

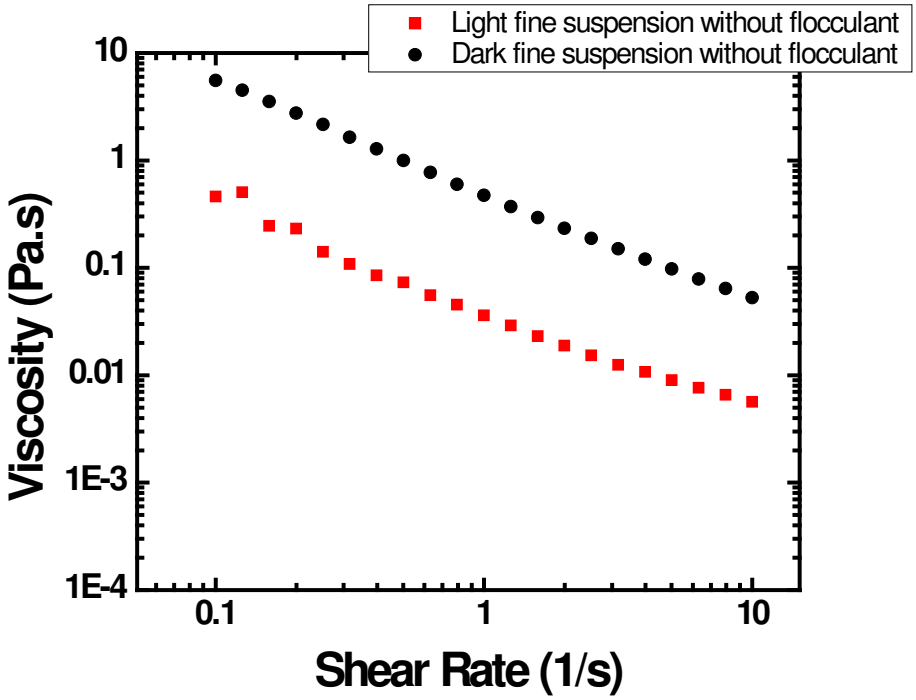

Figure 5-6 Viscosities of suspensions of 10 wt % light and dark fine particles (fractionated from WIP MFT) before flocculant addition at 25°C

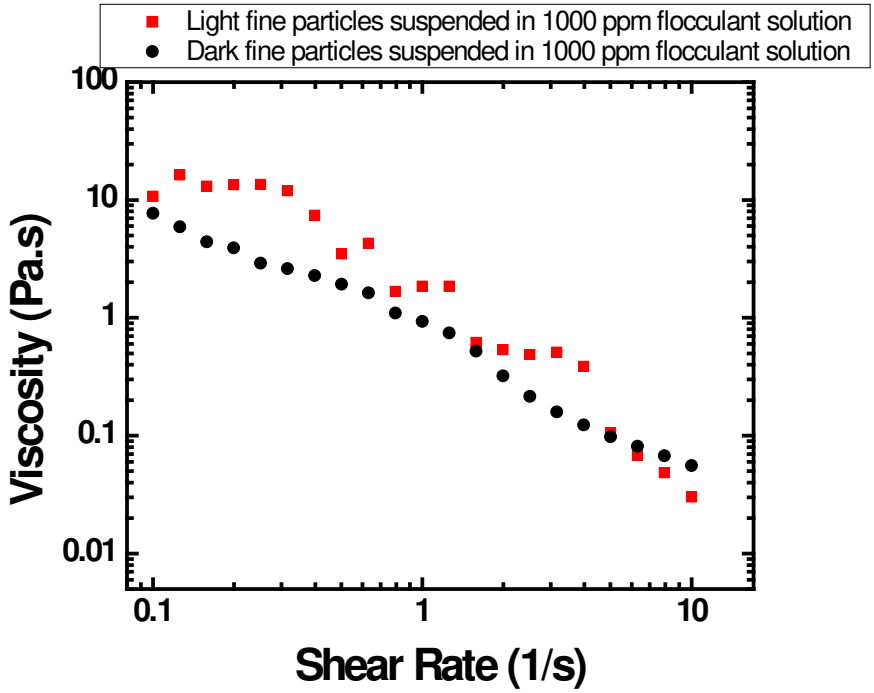

Figure 5-7 **Viscosities of suspensions of 10 wt% light and dark fine particles (fractionated from WIP MFT) in flocculant solution of 1000 ppm at 25°C**

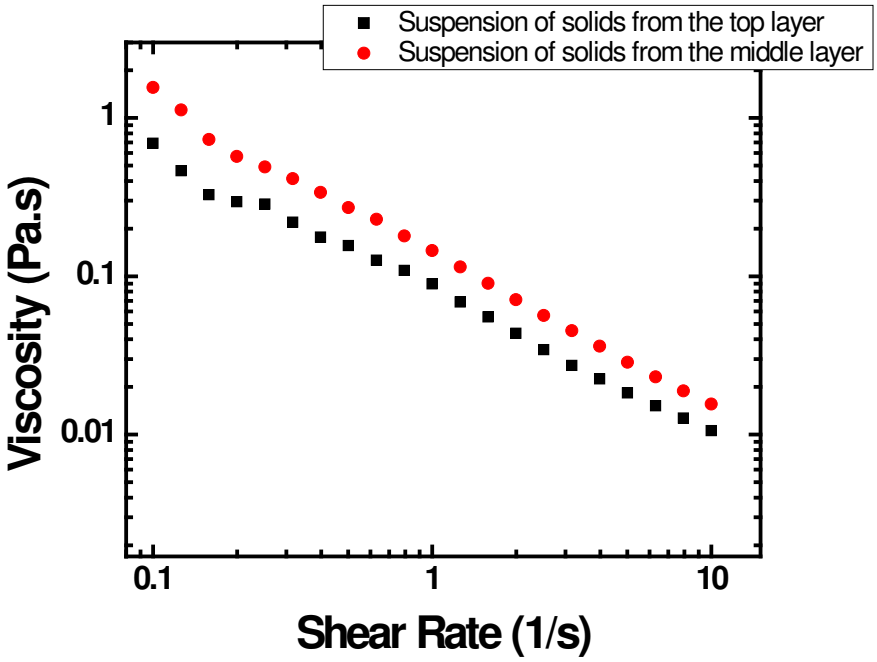

Figure 5-8 **Viscosities of suspensions of 10 wt% solid particles from the top and middle layers (separated by flocculant addition to WIP MFT) at 25°C**

5.3.2.2 Comparison of the elastic and viscous moduli of light and dark particle suspensions (without flocculant) with particles from the top and middle layers

Strain sweep test results show that the suspension of 10 wt% of dark fine particles (without flocculant) exhibit higher solid like properties ($G^{'}$) in comparison with the suspension of light fine particles (without flocculant) with the same solid concentration. The magnitude of the viscous modulus for these two fractions is similar as shown in Figure 5-9.

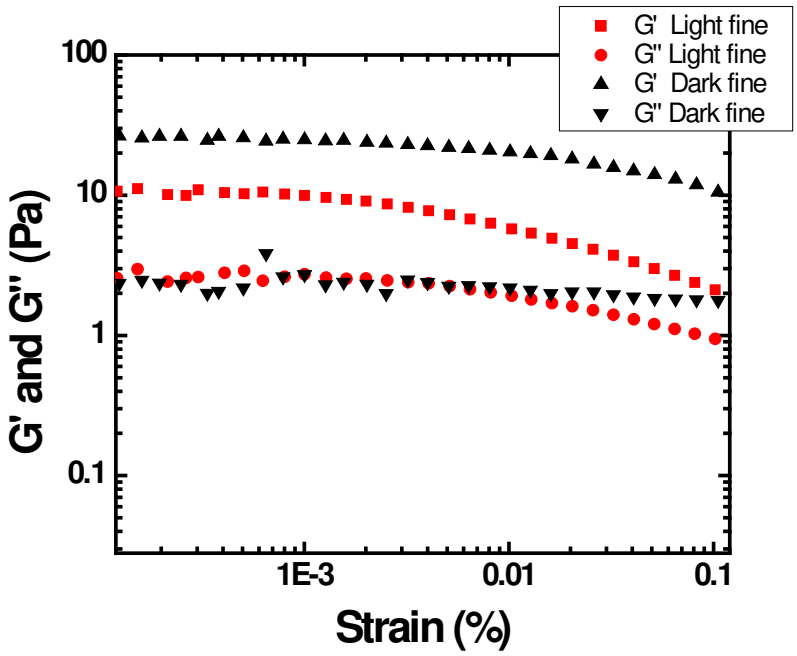

Figure 5-9 Elastic and viscous moduli of suspensions of 10 wt% light and dark fine particles (without flocculant) fractionated from WIP MFT at 25°C

A similar test was conducted for the suspensions of solid particles from the top and middle layer of the cylinder shown in Figure 4-17. The concentration of solids was adjusted to be 10 wt% in these suspensions. The results from Figure 5-10 suggest that elastic and viscous moduli of the suspensions of solids from the middle layer are higher than those for the top layer by about one order of magnitude. This finding shows that solid particles from the middle layer (which are similar to light fine particles and contain lower organic content) become more

flocculated and exhibit higher solid like properties (G') in comparison with solid particles from the top layer (which are similar to dark fine particles and contain higher organic content).

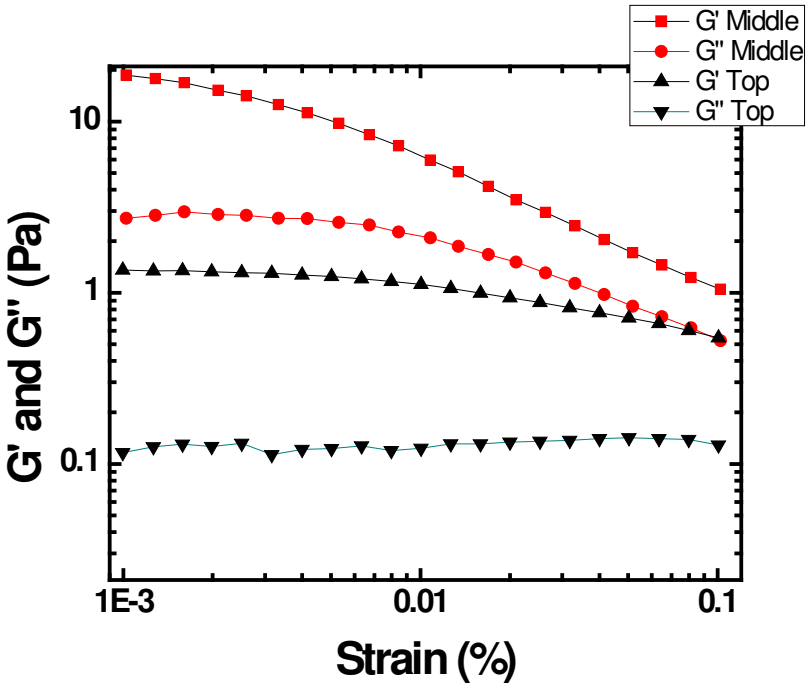

Figure 5-10 Elastic and viscous moduli of suspensions of 10 wt% solid particles from the top and middle layers (separated by flocculant addition to WIP MFT) at 25°C

5.3.2.3 Comparison of the gelation rate of light and dark fine particle suspensions (without flocculant) with suspensions of particles from the top and middle layers

Another important aspect in rheological properties of suspensions is the rate of gelation. As described in Section 2.6.1, the rate of gelation of particles can be measured by the rate of change in gelation index using H NMR system. Another method, known as time sweep tests can be used to measure the gelation rate of suspensions by using a rheometer. As mentioned in Section 2.6.3, ultra fine solid particles form a gel due to the formation of a structural network. One can measure the gelation rate of the suspensions by pre shearing them and measuring the rate

of increase in elastic modulus after the mixing is stopped. The elastic modulus of 10 wt% light and dark fine particle suspensions was measured for half hour after pre-shearing the suspension for 10 minutes at 100 rpm. Figure 5-11 shows the rate of gelation for dark and light fine particle suspensions. Result suggests the higher gelation rate of dark fine particles.

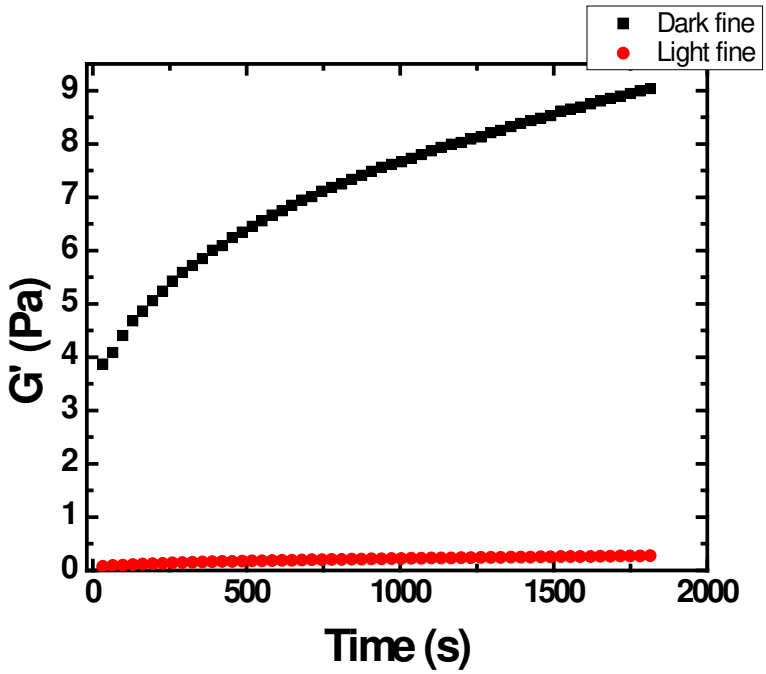

Figure 5-11 Gelation rate of suspensions of 10 wt% light and dark fine particles (without flocculant) fractionated from WIP MFT at 25°C

A similar test was conducted for the suspension of solids from the top and middle layers. Results from Figure 5-12 show that the gelation rate of the suspension of solid particles from the middle layer is higher than the top layer. Comparing the results in Figure 5-11 and Figure 5-12 suggests that after the adsorption of polymer, the solid particles containing lower amount of organic material, in the middle layer, exhibit more solid like behaviour and higher gelation rate, while in the original state, dark fine particles, containing more organic material had higher elastic modulus and gelation rate. This again is due to higher degree of flocculation in solid particles from the middle layer. These results are consistent

with the results of the viscoelasticity and viscosity measurements described in Section 5.3.2.1 and 5.3.2.2.

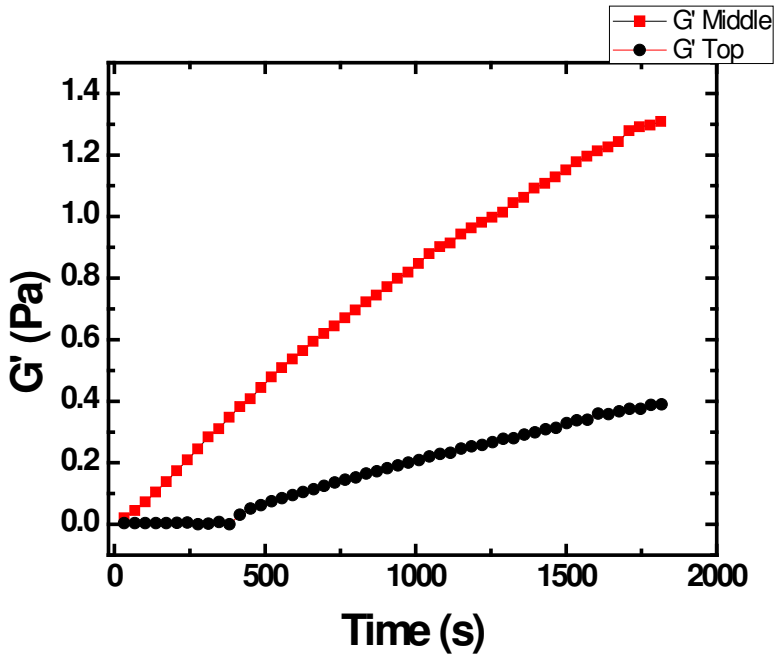

Figure 5-12 Gelation rate of suspensions of 10 wt% solid particles from the top and middle layers (separated by flocculant addition to WIP MFT) at 25°C

5.4 Adsorption of coagulant on light and dark fine particles

In the previous section of this Chapter adsorption of flocculant (Magnofloc1011) on light and dark fine particles was investigated. Coagulants can also be used in MFT treatment to improve the flocculation of particles, thus it is important to study the adsorption of coagulants on the surface of particles.

5.4.1 Zeta potential changes due to coagulant adsorption

To understand the changes in the surface charges due to the adsorption of coagulants, dark and light fine particles were dispersed in Syncrude process water. Zeta potential of suspensions of 1 wt% of these fine particles was then measured before and after addition of coagulants such as $MnCl_2$ and $CaCl_2$ using ZetaPALS instrument. The results are presented in the Table 5-3. Concentrations

of coagulant and flocculant in this table are with respect to solids in the suspension.

Table 5-3 Zeta potentials of light and dark fine particles (fractionated from WIP MFT) in different electrolytes

Zeta potential(mV)	Base	6000 ppm $MnCl_2$	1000 ppm flocculant, 6000 ppm $MnCl_2$	6000 ppm $CaCl_2$
Dark fine	-39	-28	-27	-25
Light fine	-41	-26	-27	-24

Results in Table 5-3 show that the surface charges of both dark and light fine particles decrease to almost the same extent due to electric double layer compression and/or specific adsorption of cations, changing from about -40 mV to around -25 mV for both samples. Addition of polymer prior to coagulant had little effect on zeta potential reduction. According to these results it seems that adsorption of coagulants on the surface of fine particles is not affected by their amount of organic content.

5.5 Further characterization of light and dark fine particles

So far the reasons for stability of fine particles suspended in the top layer of cylinder shown in Figure 4-17 have been discussed. It was found that higher amount of organic content and lower level of polymer adsorption are the main reasons for the lower settling rate of these types of solids in comparison with the solids from the middle layer. It was also found that the fine particles in the top and middle layers are mostly similar to the physically fractionated dark and light fine particles, thus further characterization of light and dark fine particles can enhance our knowledge about the particles in the top and middle layers. Cation exchange capacity and EDX analysis tests were conducted for light and dark fine particles for this purpose.

5.5.1 EDX analysis of light and dark fine particles

Elemental analysis of the light and dark fine particles does not show a considerable difference in the composition of the elements listed in Table 5-4.

Table 5-4 EDX analysis for light and dark fine particles fractionated from WIP MFT

Element	Light fine wt%	Dark fine wt%
Na	0	<1
Mg	1	1
Al	27	26
Si	56	52
S	1	1
K	5	7
Ca	<1	<1
Ti	2	1
Fe	9	11

5.5.2 Cation exchange capacity (CEC) measurements for light and dark fine particles

CEC is the capacity of clays for adsorbing the cations in the solution. Methylene blue analysis method was used to compare the CEC of the dark and light fine particles. In this experiment, 213.6 mg of light fine particles and 200.3 mg of dark fine particles after ashing by low temperature ashing technique were dispersed in 50 ml of 0.015 M $NaHCO_3$ and 2 ml of 10 wt% NaOH. The mixtures were mixed using a magnetic stirrer for 30 minutes until complete dispersion of the particles was achieved. During this period, sonication was applied to assist the dispersion of particles. Following the complete dispersion of the particles, 2 ml of 10 wt% H_2SO_4 was added into the slurry to make sure that the pH is lower than 3. Each sample was titrated with a 0.006N solution of methylene blue with the slurry being stirred. After addition of 1ml of the methylene blue in each stage, one drop of the mixture was placed on a Whatman #4 filter paper. Appearance of a blue

halo around the circle on the filter paper indicates the end of titration. After the appearance of the blue halo, the slurry was mixed for two more minutes without addition of any more methylene blue. If the blue halo was still present after mixing, the end of the titration was considered to be reached [44]. The end point of titration for dark and light fine particles in these cases was 11.3 ml and 7 ml of methylene blue, respectively. The CEC and surface area of the particles are calculated using the following two equations:

$$MBI(meq/100g\ solids) = \frac{(vol.MB \times normality\ of\ MB)}{weight.solids, g} \times 100 \qquad \text{Eq 5.1}$$

$$SA(m^2/g) = MBI \times 130 \times 0.0602 \qquad \text{Eq 5.2}$$

The MBI (methylene blue index) for dark and light fine particles are 32.9 meq/100 g solids and 19.2 meq/100 g solids respectively and SA (specific surface area) are 257.9 m^2/g and 150. 5 m^2/g for dark and light fine particles. The higher surface areas of dark fine particles than light fine particles after removal of organic material with LTA, suggests smaller average particle size or more porous structure in this fraction.

This finding can also explain the lower settling rate of the fine particles in the top layer of cylinder shown in Figure 4-17. Dark fine particles are either smaller or have higher porosity than the light fine particles after removal of organic matters from their surfaces. Without removal of organic matters the dark fine particles appear to have similar particle size to the light fine particles as shown in Figure 3-6. Thus the dark fine particles with higher amount of organic content should have lower density than the light fine particles. Similarly the particles in the top layer settle down slower due to their lower density.

5.6 Summary

The effect of organic content in sedimentation of fine particles in MFT suspension which was treated with flocculant was studied in this Chapter. It was found that a fraction of fine particles with higher amount of organic matters (solids from the top layer of Figure 4-17) have lower settling rate in comparison with another fraction of fines with the same size but lower organic content (solids from the middle layer). Comparing the rheological properties of these fine solids with the physically fractionated fine particles from this MFT sample (light and dark fine particles) showed the lower level of polymer adsorption on the solids with high organic content (solids from the top layer and dark fine particles) than those with low organic content (solids from the middle layer and light fine particles). Thus it seems that high amount of organic content and low level of polymer adsorption are the main reasons for stability of fine solid particles in the top layer of cylinder shown in Figure 4-17.

6 Conclusion

6.1 Problem review

Oil sands ores are one of the most reliable sources of liquid fossil fuel energy in North America. In 2007, Canada supplied about 13% of the imported oil by exporting 1.34 billion barrels of crude oil to US. In addition, 1 out of 13 jobs in Alberta is directly related to energy. It is also important to note that every dollar invested in oil sands creates $9 of economic activity. These and other similar facts justify the ever increasing efforts and investments in oil sands technology [45].

Sustainable development in oil sands industry requires cautious protection of the air, land and water. Development in technologies related to these areas is an ongoing process. Examples of these technologies are carbon capture and storage (CCS) technology for air protection and CT and paste technology for land reclamation. Regarding the water protection, strict limits have been set for industrial water use through Alberta's Water Management Framework for the Lower Athabasca River. Collectively all oil sands projects including the existing and approved ones are allowed to withdraw about three percent of average annual flow of the river. Due to these restrictions many companies recycle about 80%-90% of the water they use.

An important stage in recycling the water is the solid-liquid separation as the recycled water should meet certain criteria of chemistry and solid content in order to be used in the plant. Solid-liquid separation by means of flocculation of solid particles in thickeners is used by some companies such as Albian in Muskeg River Mine. Considerable amounts of research on the flocculation and sedimentation of particles have been conducted over the years.

This project focused on the characterization of the most stable part of fine solid particles in mature fine tailings in the context of their sedimentation in different

water chemistry and different dilution and their rheological behaviour. Different characterization techniques such as XRD, for mineral analysis, XPS and EDX, for surface elemental analysis, FTIR and TGA, for organic contents measurements, have been used for this purpose.

6.2 Important findings from this study

i. MFT dilution has a profound effect on settling of solid particles. Diluting MFT samples by deionized water helps the settling of solid particles due to changing of water chemistry and concentration effect. Dilution also improves the initial settling rate of the particles.

ii. Different layers of solid particles in MTF respond differently to macromolecule flocculant in the context of flocculation and settling. This response does not only depend on the size of particles as described in [35] but also on the presence of organic matter. Regarding the size of the particles, as the particles become finer their settling rate decreases. Flocculant assisted coagulation of fine particles (FC treatment) results in formation of super flocs with high water to solid ratio. Regarding the presence of organic matter, which is bonded to some fraction of fine particles, it has been noted that organic-rich fine particles have lower settling rate than fine particles with low amount of organic matters as they adsorb the macromolecules of polymer to a lesser extent. This might be due to the lower affinity of hydrophobic organic matters on the surface of these particles to the Magnofloc polymer.

iii. Although dark fine particles have greater elastic modulus and viscosity than light fine particles in the original state, treating the sample with polymer, Magnofloc 1011, reverse the situation.

iv. Ultra fine particles containing a higher amount of organic matter i.e. dark fines are either smaller in size or have more porous structure in comparison with those ultra fine particles with less amount of organic matter i.e. light fines.

References

[1] Masliyah, J.H., and Gray, M.R., 2008, "Extraction and Upgrading of Oil Sands Bitumen", Chap. A1 pp. 1.

[2] Nelson, L.R., Gulley, J.R., and MacKinnon, M., 1995, "Environmental Issues on Reclamation of Oil Sands Fine Tails", 6th UNITAR Conference, Houston, TX.

[3] MacKinnon, M., 1989, "Development of Tailings Pond at Syncrude's Oil Sands Plant: 1978-1987", AOSTRA Journal of Research. 5 pp. 109.

[4] Rogers, M.E., Ferguson, D., and MacKinnon, M., 1996, "Water Management Challenges at the World's Largest Integrated Oil Sands Mining and Refining Complex", The NACE Int. Ann. Conference and Exposition, Paper #568, Denver, CO.

[5] Masliyah, J.H., and Gray, M.R., 2008, "Extraction and Upgrading of Oil Sands Bitumen", Chap. B6 pp. 1.

[6] Yong, R.N., and Sethi, A.J., 1978, "Mineral Particle Interaction Control of Tar Sand Sludge Stability", Journal of Canadian Petroleum Technology. (Oct-Dec) pp. 76.

[7] Majid, A., and Sparks, B.D., 1996, "Role of Hydrophobic Solids in the Stability of Oil Sands Fine Tailings", Fuel. 75(7) pp. 879-884.

[8] Fine Tailings Fundamentals Consortium, 1995, "Advances in Oil Sands Tailings Research", Alberta Dept. of Energy, Edmonton.

[9] Allan, A.R., and Sanford, E.D., 1974, "Information Services 65 Alberta Research Council", pp. 103.

[10] Tu, Y., O'Carroll, J.B., Kotlyar, L.S., Sparks, B.D., Ng, S., Chung, K.H., and Cuddy, G., 2005, "Recovery of Bitumen from Oil Sands: Gelation of Ultra-Fine Clay in the Primary Separation Vessel", Fuel. 84(6) pp. 653-660.

[11] Kotlyar, L.S., Sparks, B.D., Lepage, Y., and Woods, J.R., 1997, "Effect of Particle Size on Clay Flocculation Behavior of Ultra-Fine Clays in Salt Solutions", Clay Minerals. 33 pp. 103.

[12] Barnes, H.A., Hutton, J.F., and Walters, K., 1989, "An Introduction to Rheology", Elsevier Science Ltd, UK.

[13] Majid, A., and Ripmeester, J.A., 1985, "Recovery of Heavy Metal Minerals from Oil Sands and Oil Sands Tailings by Oil Phase Agglomeration", Third UNITAR/UNDP Conference, Long Beach, CA.

[14] Sparks, B.D., Kotlyar, L.S., O'Carroll, J.B., and Chung, K.H., 2003, "Athabasca Oil Sands: Effect of Organic Coated Solids on Bitumen Recovery and Quality", Journal of Petroleum Science and Engineering. 39(3-4) pp. 417.

[15] Majid, A., Argue, S., Boyko, V., Pleizier, G., L'Ecuyer, P., Tunney, J., and Lang, S., 2003, "Characterization of Sol–Gel-Derived Nano-Particles Separated from Oil Sands Fine Tailings", Colloids and Surfaces A: Physicochemical and Engineering Aspects. 224(1-3) pp. 33-44.

[16] Brown, G., 1961, "The X-Ray Identification and Crystal Structures of Clay Minerals", Mineralogical Society, London.

[17] Kotlyar, L.S., Kodama, H., Sparks, B.D., and Gratten-Bellew, P.E., 1987, "Non-Crystalline Inorganic Matter-Humic Complexes in Athabasca Oil Sands and their Relationship to Bitumen Recovery", Applied Clay Science. 2 pp. 253.

[18] Matthews, J.G., Shaw, W.H., Mackinnon, M.D., and Cuddy, R.G., 2002, "Development of Composite Tailings Technology at Syncrude", International Journal of Surface Minning, Reclamation and Environment. 16(1) pp. 24.

[19] Cymerman, G., Kowang, T., Lord, T., Hamza, H., and Xu, Y., 1999, "Thickening and Disposal of Fine Tails from Oil Sand Processing", The Third UBC-McGill Int. Sym. Fund. of Mineral Processing (CIM), Quebec City.

[20] Mikula, R.J., Kasperski, K.L., Burns, R.D., and Mackinnon, M.D., 1996, "Suspensions: Fundamentals and Applications in Petroleum Industry", American Chemical Society Books, Washington, DC, pp. 677.

[21] Vorob'ev, P.D., Krut'ko, N.P., Vorob'eva, E.V., and Strnadova, N., 2008, "Successive Adsorption of Polyacrylamide Compounds from Electrolyte Solutions on the Surface of Kaolinitic Clay Particles", Colloid Journal. 20(2) pp. 148.

[22] Gregory, R., 1987, "Flocculation by Polymers and Polyelectrolyte in Solid/Liquid Dispersions", Academic Press, New York.

[23] Elimelech, M., 1995, "Particle Deposition and Aggregation: Measurement, Modeling and Simulation", Butterworth-Heinemann, Oxford.

[24] Lin, M.Y., Lindsay, H.M., Weitz, D.A., Ball, R.C., Klein, R., and Meakin, P., 1990, "Universal Reaction-Limited Colloid Aggregation", Physical Review. 41(4) pp. 2005.

[25] Mandelbrot, B.B., 1983, "The Fractal Geometry of Nature", W.H. Freeman & Co, New York.

[26] Zhou, Y., and Franks, G.V., 2006, "Flocculation Mechanism Induced by Cationic Polymers Investigated by Light Scattering", Langmuir. 22 pp. 6775.

[27] Oles, V., 1992, "Shear-Induced Aggregation and Breakup of Polystyrene Latex Particles", Journal of Colloid and Interface Science. 154(2) pp. 351-358.

[28] Berhane, I., Sternberg, R.W., Kineke, G.C., Milligan, T.G., and Kranck, K., 1997, "The Variability of Suspended Aggregates on the Amazon Continental Shelf", Continental Shelf Research. 17(3) pp. 267-285.

[29] Sworska, A., Laskowski, J.S., and Cymerman, G., 2000, "Flocculation of the Syncrude Fine Tailings: Part I. Effect of pH, Polymer Dosage and Mg2+ and Ca2+ Cations", International Journal of Mineral Processing. 60(2) pp. 143-152.

[30] Hogg, R., 1999, "Polymer Adsorption and Flocculation", The Third UBC-McGill Int.Sym.Fund. of Mineral Processing (CIM), Quebec City.

[31] Hogg, R., 1999, "The Role of Polymer Adsorption Kinetics in Flocculation", Colloids and Surfaces A: Physicochemical and Engineering Aspects. 146(1-3) pp. 253-263.

[32] Kitchener, J.A., 1978, "Flocculation in Mineral Processing", Sitjthoff & Noordhoff, Holland.

[33] Sworska, A., Laskowski, J.S., and Cymerman, G., 2000, "Flocculation of the Syncrude Fine Tailings: Part II. Effect of Hydrodynamic Conditions", International Journal of Mineral Processing. 60(2) pp. 153-161.

[34] Banisi, S., and Yahyaei, M., 2008, "Feed Dilution Based Design of a Thickener for Refuse of a Coal Preparation Plant", International Journal of Coal Preparation and Utilization. 28(4) pp. 201.

[35] Yuan, X.S., and Shaw, W., 2007, "Novel Processes for Treatment of Syncrude Fine Transition and Marine Ore Tailings", The Canadian Metallurgical Quarterly. 46(3) pp. 265.

[36] Mikula, R.J., Munoz, V.A., and Omotoso, O., 2008, "Centrifuge Options for Production of Dry Stackable Tailings in Surface Mined Oil Sands Tailings Management", Canadian International Petroleum Conference, Calgary, AB.

[37] Macosko, C.W., 1994, "Rheology-Principles, Measurements and Applications", Wiley-VCH, New York.

[38] Van Olphen, H., 1991, "An Introduction to Clay Colloid Chemistry", Krieger Publishing Company, Malabar, FL.

[39] Angle, C.W., Zrobok, R., and Hamza, H.A., 1993, "Surface Properties and Elasticity of Oil-Sands-Derived Clays found in a Sludge Pond", Applied Clay Science. 7(6) pp. 455-470.

[40] Tatterson, G.B., 1991, "Fluid Mixing and Gas Dispersion in Tanks", McGraw-Hill, New York.

[41] Eshel, G., Levy, G.J., Mingelgrin, U., and Singer, M.J., 2004, "Critical Evaluation of the use of Laser Diffraction for Particle Size Distribution Analysis", Soil Science Society of America Journal. 68(3) pp. 736.

[42] Parker, S.P., 1988, "Spectroscopy Source Book", McGraw-Hill, New York.

[43] Callister, W.D., 1994, "Materials Science and Engineering – an Introduction", Wiley & Sons, New York.

[44] Hang, P.T., and Brindley, G.W., 1970, "Methylene Blue Adsorption by Clay Minerals-Determination of Surface Areas and Cation Exchange Capacities", Clays and Clay Minerals. 18(4) pp. 203.

[45] "Alberta's Oil Sands: Protecting the Environment", www.oilsands.alberta.ca.